iScience

Article

Distinct role of primate DLPFC and LIP in hierarchical control of learned saccade sequences

Graphical abstract

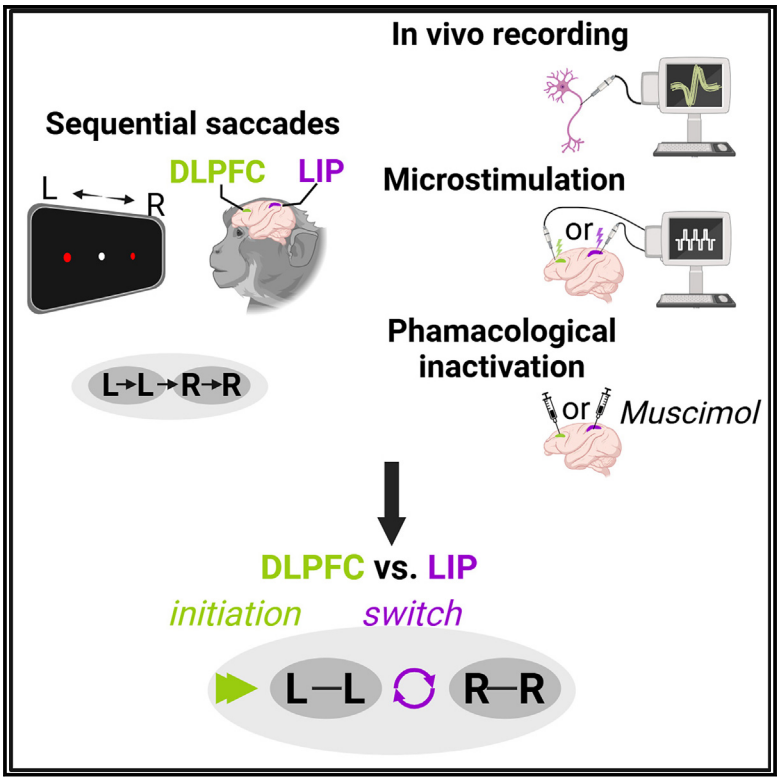

Authors

Qingjun Wang, Binchao Shi, Jing Jia, Jingyu Hu, Haoran Li, Xin Jin, Aihua Chen

Correspondence

xjin@bio.ecnu.edu.cn (X.J.), ahchen@brain.ecnu.edu.cn (A.C.)

In brief

Biological sciences; Physiology; Neuroscience

Highlights

- DLPFC and LIP encoded hierarchical levels of learned saccade sequences differently
- Inactivation in DLPFC delayed the initiation of the sequences
- Microstimulation of LIP affected the switch between subsequences
- DLPFC and LIP play distinct yet complementary roles in saccade sequences

Wang et al., 2025, iScience *28*, 111694
January 17, 2025
https://doi.org/10.1016/j.isci.2024.111694

CellPress

iScience

CellPress
OPEN ACCESS

Article

Distinct role of primate DLPFC and LIP in hierarchical control of learned saccade sequences

Qingjun Wang,[1,4] Binchao Shi,[1,4] Jing Jia,[1] Jingyu Hu,[1] Haoran Li,[1] Xin Jin,[1,2,3,*] and Aihua Chen[1,3,5,*]
[1]Key Laboratory of Brain Functional Genomics (Ministry of Education), East China Normal University, Shanghai 200062, China
[2]New Cornerstone Science Laboratory, Center for Motor Control and Disease, East China Normal University, Shanghai 200062, China
[3]NYU-ECNU Institute of Brain and Cognitive Science, New York University Shanghai, Shanghai 200062, China
[4]These authors contributed equally
[5]Lead contact
*Correspondence: xjin@bio.ecnu.edu.cn (X.J.), ahchen@brain.ecnu.edu.cn (A.C.)
https://doi.org/10.1016/j.isci.2024.111694

SUMMARY

Learned action sequences are suggested to be organized hierarchically, but how the various hierarchical levels are processed by different cortical regions remains largely unknown. By training monkeys to perform heterogeneous saccade sequences, we investigated the role of the dorsolateral prefrontal cortex (DLPFC) and the lateral intraparietal cortex (LIP) in sequence planning and execution. The electrophysiological recording revealed that sequence-level initiation information was mostly signaled by DLPFC neurons, whereas subsequence-level transition was largely encoded by LIP neurons. Although electrical microstimulation on DLPFC weakly affected sequence performance, inactivating DLPFC significantly increased the initiation latency of the entire sequences, indicating that DLPFC was involved in the sequence initiation. In contrast, either microstimulation or inactivation of area LIP caused improper switches between subsequences, suggesting that LIP played a role in subsequence switch. Overall, these results demonstrated that frontal and parietal cortices play distinct yet complementary roles in controlling learned saccade sequences.

INTRODUCTION

Action sequences contribute to numerous daily behaviors, such as writing, speaking, or playing instruments.[1] Nowadays, learned action sequences are suggested to be organized in a hierarchical model with individual actions first organized into subsequences, then the sequence.[2–5] However, the underlying mechanism of hierarchical organization of sequence in the brain remains largely unclear and needs further investigation.

The sequential saccade task provides a good behavior model to study the neural mechanism of the action sequence due to its simplicity with fewer degrees of freedom.[6] The neural pathways of the single saccade were also well understood, and several brain areas had been identified to participate in these neural circuits, including the primary visual cortex (V1), the lateral intraparietal cortex (LIP), the dorsolateral prefrontal cortex (DLPFC), the supplementary eye field (SEF), the frontal eye field (FEF) and superior colliculus (SC).[7,8] Among these areas, FEF was supposed to play a role during sequential saccades as it showed predictive coding for future targets during sequence execution,[9,10] and parallel programming activities for multiple sequential saccades.[10] Our previous study also observed that FEF neurons dynamically encoded the saccade sequence, and pharmacological inactivation of FEF impaired the monkey's saccade performance. However, the microstimulation-evoked saccades in FEF did not alter the sequence structure, indicating that it might be at a lower level in hierarchical control and close to the motor output.[11] Then, a related question is raised about which brain areas contribute to the higher levels of controlling sequence structure within the hierarchical organization.

DLPFC might be a possible higher-level candidate with direct projection to FEF.[8,12] Several studies reported that DLPFC neurons were involved in the initiation of the whole sequence: it has been previously reported that when monkeys made sequential saccades by following successively presented visual targets, prefrontal cortex (PFC) neurons exhibited excitatory responses at the beginning and endpoint of sequence[13]; In addition, for the memory-guided motor sequence, lateral PFC neurons held the temporal structure information, and activated before the execution of specific sequences,[14] or sequence categories.[15] These studies indicate that DLPFC had a neuronal correlation with the initiation of the hierarchically organized sequences, a sign of encoding at the sequence level. On the other hand, since different hierarchical levels of the sequence were usually coded in a mixed way in the premotor and parietal cortices,[16] whether DLPFC also encodes other hierarchical levels (e.g., the subsequence level and element level) remains unexplored. More importantly, whether DLPFC causally contributes to the sequence organization needs investigation.

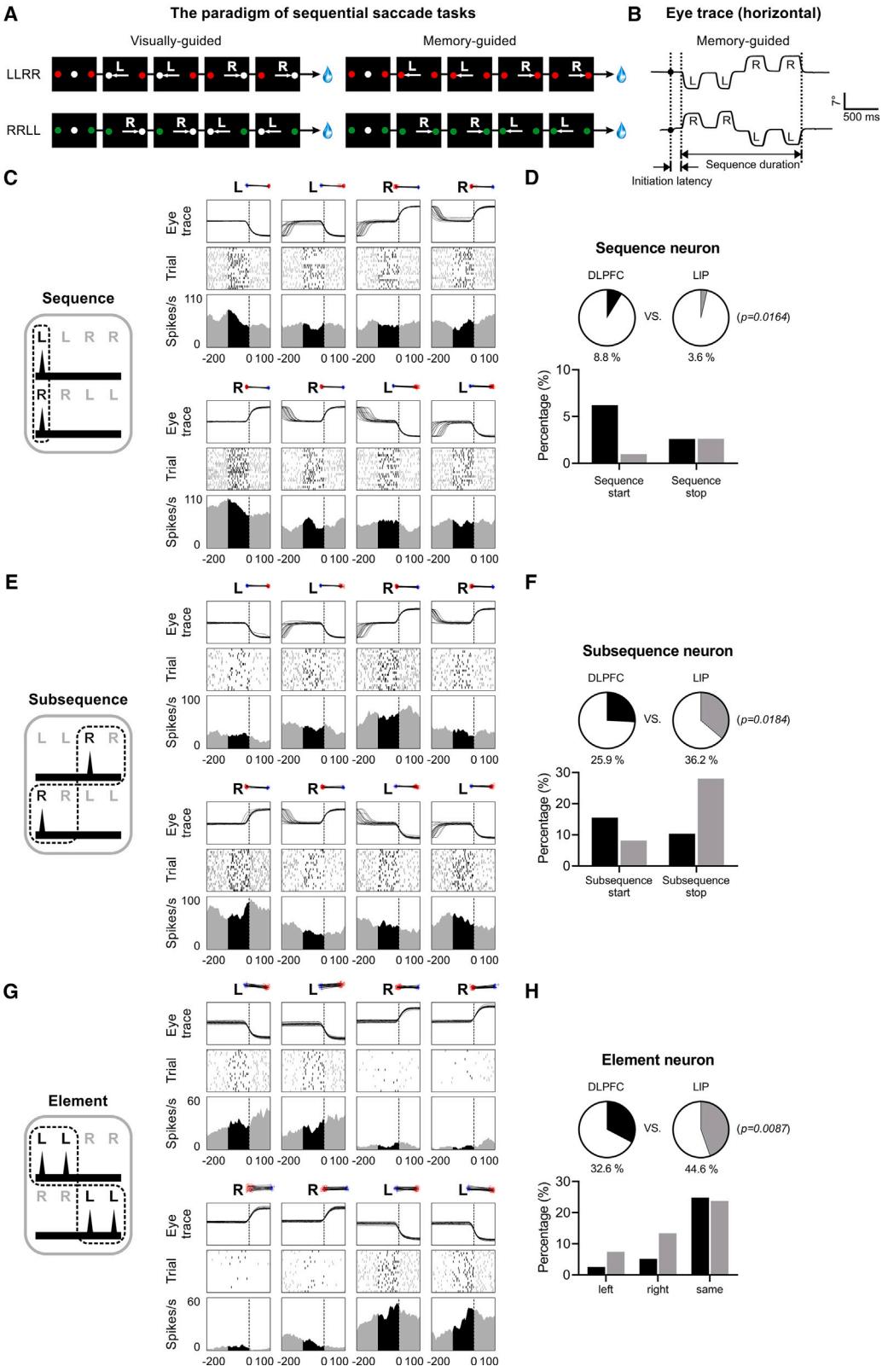

(legend on next page)

Besides DLPFC, fMRI studies in humans found that the parietal cortex hierarchically represented sequence and chunk (similar to the subsequence mentioned above) layers in motor sequences, implying a high-level encoding in the sequence hierarchy.[16] Furthermore, the activity of the parietal cortex increased with the complexity of the sequence,[17] and it has been speculated that this enhanced activity may be related to the increase in the number of subsequences/chunks.[18] Thus, LIP might be another candidate for the high-level sequential saccade task. However, previous studies mainly focus on fMRI responses, and the encoding characteristic of single LIP neurons at the subsequence level as well as the other hierarchical levels is unclear. Also, whether there is a causal relationship between these neuronal encodings of LIP and the hierarchical control of sequence is largely unknown.

In the current study, we explored the neuronal responses and causal roles of DLPFC and LIP in the sequential saccades. We trained monkeys to perform a set of learned hierarchically organized saccade sequences (Left-Left-Right-Right, i.e., LLRR, and Right-Right-Left-Left, i.e., RRLL, see STAR Methods and Figure 1A),[5,11] which consisted of individual elements (left, and right), intermediate subsequence (left-left, and right-right), and overall sequence (left-left-right-right, and right-right-left-left). Extracellular recording was performed to examine the characteristics of the neuronal representation. We found that neurons in DLPFC and LIP encoded hierarchical levels of sequences differently. To further investigate whether the sequentially related responses causally contribute to the behavior, we first applied electrical microstimulation experiments and found that microstimulating DLPFC just affected the sequence performance weakly. Since microstimulation might only affect a subset of neurons that contribute to sequence, the causal roles of the whole area of DLPFC were further explored by reversible inactivation. The inactivation result revealed the crucial role of DLPFC in sequence initiation. Notably, both microstimulation and inactivation on LIP significantly altered the subsequence switch. Overall, our results uncovered distinct functions of DLPFC and LIP, which provides a basis for understanding the mechanism of the hierarchical organization of learned action sequences.

RESULTS

DLPFC and LIP differently encode sequence-, subsequence- and element-level of saccade sequences

To explore the roles of DLPFC and LIP in the hierarchical organization of saccade sequences, we trained five monkeys (monkeys C, E, F, I, M) to learn two hierarchically organized sequential saccade tasks, Left-Left-Right-Right (LLRR) and Right-Right-Left-Left (RRLL) (Figures 1A and 1B, see STAR Methods for details). After training, monkeys could skillfully perform the learned LLRR and RRLL sequential saccade tasks (Figure S1), then we performed electrophysiological recordings and examined the neural coding of sequential hierarchy in the memory-guided sequence.

In DLPFC, 389 cells were recorded in two monkeys totally (monkey I: left hemisphere, n = 177, right hemisphere, n = 99; monkey C: right hemisphere, n = 113), and 205 cells with both LLRR and RRLL tasks tested were included for further analysis. In LIP, 455 cells (monkey E: left hemisphere, n = 136; monkey F: left hemisphere, n = 159; monkey M: right hemisphere, n = 160) were recorded, and 443 cells with both LLRR and RRLL tasks (Figure S2). Details for brain area localization and neuron distribution were described in STAR Methods and Figure S2. We found the majority of these recorded cells (94.1%, 193/205 in DLPFC; 69%, 307/443 in LIP) were pre-saccadic cells, whose firing rates in pre-saccadic epochs were significantly different from baseline ($p < 0.01$, Wilcoxon rank-sum test). Based on our previous studies in the sequence hierarchy classification,[5,11] these pre-saccadic neurons were further classified into Sequence, Subsequence, and Element neurons (see STAR Methods for details).

An example Sequence-level neuron is shown in Figure 1C, with a preference for the first (1^{st}) saccade for both LLRR and RRLL sequences. The neuronal firing rate of the 1^{st} saccade in the LLRR task is 59.41 spks/s, which is higher than the other three saccades (1^{st} vs. 2^{nd}, p = 0.2559, 1^{st} vs. 3^{rd}, p = 0.1068, 1^{st} vs. 4^{th}, p = 0.4807, one-way ANOVA). The 1^{st} saccadic firing rate in the RRLL task is 84.65 spks/s, significantly higher than the other three (1^{st} vs. 2^{nd}, p = 0.0032, 1^{st} vs. 3^{rd}, p = 0.0124, 1^{st} vs. 4^{th}, p = 0.0032, one-way ANOVA). As this neuron fired to the start of the sequences, it was named the ***"Sequence start"*** neuron. Besides, neurons that showed selectivity to the stop (the last/4^{th} center-out saccade) for both LLRR and RRLL sequences, were considered ***"Sequence stop"*** neurons. Among the population, 8.8% (17/193) of DLPFC neurons showed such sequence-level activation, and most of them (n = 12) were "Sequence start" neurons. However, Sequence neurons in LIP counted for 3.6% (11/307), significantly lower than that in DLPFC (p = 0.0164; Fisher's exact test), and the majority of them were "Sequence stop" neurons (n = 8) (Figure 1D).

An example Subsequence-level neuron is illustrated in Figure 1E. This neuron prefers the first saccade (1^{st} R) in the RRLL

Figure 1. DLPFC and LIP neurons represent different hierarchical levels of saccade sequences

(A) Schematic of visually guided and memory-guided sequential saccade tasks for LLRR (top) and RRLL (bottom).

(B) Samples of monkey's eye trace on performing a single trial of memory-guided saccade sequence: LLRR (top) and RRLL (bottom). Initiation latency is defined as the period between the appearance of the trial start cues and the onset of the first saccade. Sequence duration is defined as the total time to perform a whole memory-guided sequence.

(C) Representative Sequence neuron showing start signal. Left: schematic of neural activity. Right: example neuron recorded in DLPFC. 2D gaze plots (start point is in red, stop point is in blue) are shown in the top. Each curve indicates an eye trace in a trial. Each raster indicates a spike, and each row represents a trial, n = 20 repetitions. Time zero indicates saccade onset.

(D) Proportion of Sequence neurons. Top: comparison between DLPFC (black) and LIP (gray). Bottom: proportions of Sequence start and Sequence stop neurons.

(E and F) Same as (C-D), but for Subsequence neuron.

(G and H) Same as (C-D), but for Element neuron. Fisher's exact test was conducted for the DLPFC vs. LIP comparison in (D), (F), and (H). See also Figures S1–S3.

sequence, but not in the LLRR sequence. Instead, it shows a preference for the 3rd saccade but the 1st R in the LLRR sequence. In other words, it prefers the 1st saccade in the RR subsequence (1st R vs. 2nd R, LLRR: 60.4 vs. 30.69 spks/s, p = 0.0005; RRLL: 65.84 vs. 31.68 spks/s, $p < 0.0001$, one-way ANOVA). As this neuron significantly responds to the 1st saccade of the subsequence, we also call it the ***"Subsequence start"*** neuron. Correspondingly, neurons that prefer the 2nd saccade are classified as ***"Subsequence stop"*** neurons. Across the neuron population (Figure 1F), 25.9% (50/193) of DLPFC neurons had a subsequence-level activation, and the majority of them (n = 30) were ''Subsequence start'' neurons. Differently, the percentage of Subsequence neurons in LIP was significantly higher than in DLPFC (LIP: 36.2%, p = 0.0184, Fisher's exact test), and most of them were ''Subsequence stop'' neurons (n = 86).

In contrast to the Sequence- and Subsequence-level neurons, Element-level neurons show similar preferences for the same saccade components (e.g., 1st L vs. 2nd L, or 1st R vs. 2nd R), rather than prefer a specific rank of saccade. An Element neuron example that prefers the left saccades is shown in Figure 1G: the average firing rate of left saccades is 28.21 spks/s, significantly higher than the average firing rate of right saccades (3.71 spks/s, $p < 0.0001$, paired t-test) in the LLRR task. In addition, there is no significant difference in firing rates between the two same-direction saccades (1st L vs. 2nd L, p = 0.9911; 1st R vs. 2nd R, p = 0.9712, one-way ANOVA). A similar phenomenon is observed in the RRLL task: the average firing rate for leftward saccades (29.21 spks/s) is significantly higher than that for rightward saccades (10.89 spks/s, $p < 0.0001$, paired t-test), and the firing rates between the two leftward saccades are similar (1st L vs. 2nd L, p = 0.4632, one-way ANOVA). Accordingly, this cell is classified as an ***"Element left"*** neuron. Cells that show selectivities to the rightward saccades are named ***"Element right"*** neurons, and cells that exhibit no direction preference (consistently activated for every saccade) are considered ***"Element same"*** neurons. Among the neuron population, 32.6% (63/193) of DLPFC neurons showed element-level activation (Figure 1H), which was significantly lower than that in LIP (44.6%, p = 0.0087, Fisher's exact test).

Neurons that did not follow the above criteria were named Unclassified neurons, which encode various other aspects of information in the task. The relevant examples and proportions in DLPFC (32.6%, 63/193) and LIP (15.6%, 48/307) are shown in Figure S3.

Overall, Sequence-, Subsequence-, and Element-level neurons coexisted in DLPFC and LIP. However, DLPFC showed more representation at the sequence level than LIP, and most Sequence neurons in DLPFC had peak activity to the sequence start, implying that DLPFC might encode an initial signal in the sequence hierarchy. On the contrary, LIP exhibited more encoding at the subsequence level than DLPFC, with a specific representation of the ''stop'' of the subsequence.

DLPFC encodes the "start" of the contralateral subsequence and LIP signals the "stop" of the ipsilateral subsequence

Since Subsequence neurons counted a large proportion in both DLPFC and LIP, we further compared the response characteristics of these neurons to explore the difference between these two areas. For both LLRR and RRLL, there were two types of subsequences: LL subsequence and RR subsequence. Thus, the ***"Subsequence start"*** neurons had two categories: ***"LL start"*** and ***"RR start"*** neurons; the ***"Subsequence stop"*** neurons could also be divided into ***"LL stop"*** and ***"RR stop"*** neurons. Examples from these different groups are illustrated in Figures 2A–2D, respectively. For Subsequence stop neurons, we performed additional analysis to distinguish whether the mean firing rate of the second saccade within the subsequence primarily reflects the post-saccadic activity of the preceding saccade or the pre-saccadic activity of the upcoming saccade (see STAR Methods for details), then excluded neurons that relevant to the preceding saccade (DLPFC, n = 5; LIP: n = 33).

The example ''LL start'' neuron is shown in Figure 2A, it prefers the 1st L within the LL subsequence (1st L vs. 2nd L, LLRR: 52.97 vs. 22.77 spks/s, $p < 0.0001$; RRLL: 24.75 vs. 10.89 spks/s, p = 0.0216, one-way ANOVA). If we consider the encoding characteristic of subsequence neurons related to the recording hemisphere, this neuron was recorded from the right DLPFC, it's also a ***"Contralateral start"*** neuron. The example in Figure 2B is an ''RR start'' neuron (the same neuron in Figure 1E). Since it was recorded from the left DLPFC, it is also a ''Contralateral start'' neuron.

An ''LL stop'' neuron that exhibits a preference for the 2nd L within the LL subsequence (1st L vs. 2nd L, LLRR: 36.6 vs. 49.8 spks/s, p = 0.0184; RRLL: 72.3 vs. 99.5 spks/s, p = 0.0242, one-way ANOVA) is shown in Figure 2C, it is from the left LIP and also called ***"Ipsilateral stop"***. The ''RR stop'' neuron (1st R vs. 2nd R, $p < 0.0001$; RRLL: $p < 0.0001$, one-way ANOVA) recorded in the right DLPFC is shown in Figure 2D (also called ''Ipsilateral stop'').

The distribution ratio of Subsequence neurons was summarized in Figure 2E. Results showed that in the left DLPFC (Figure 2E, top left), about half of the Subsequence neurons were ''Contralateral start'' neurons (60%, 18/30), and 20% (6/30) were ''Ipsilateral stop'' neurons. Besides, the ''Contralateral stop'' and ''Ipsilateral start'' neurons were pooled together as ''Others'', and counted for 20% (6/30). A similar phenomenon was found in the right DLPFC (Figure 2E, top right): ''Contralateral start'' neurons accounted for the largest proportion (60%, 9/15), then the proportion of ''Ipsilateral start'' neurons was 13.3% (2/15). Thus, DLPFC neurons primarily encoded the ''start'' signal of the subsequences contralateral to their recording hemisphere.

Different from DLPFC, most Subsequence neurons in the left LIP (Figure 2E, bottom left) were ''Ipsilateral stop'' neurons (59.3%, 35/59), and 20.3% (12/59) were ''Contralateral start'' neurons. In the right LIP (Figure 2E, bottom right), ''Ipsilateral stop'' neurons (42.1%, 8/19) and ''Contralateral start'' neurons (47.4%, 9/19) were dominant respectively. These results indicated that LIP mainly exhibited the ''stop'' signal of the ipsilateral subsequence.

On the other hand, we noticed that such representation in DLPFC and LIP had a common feature: encoding the ''Ipsilateral stop'' and ''Contralateral start'' at the subsequence level. This implied that DLPFC or LIP might play a role during the subsequence switch: facilitating the stop of the ipsilateral

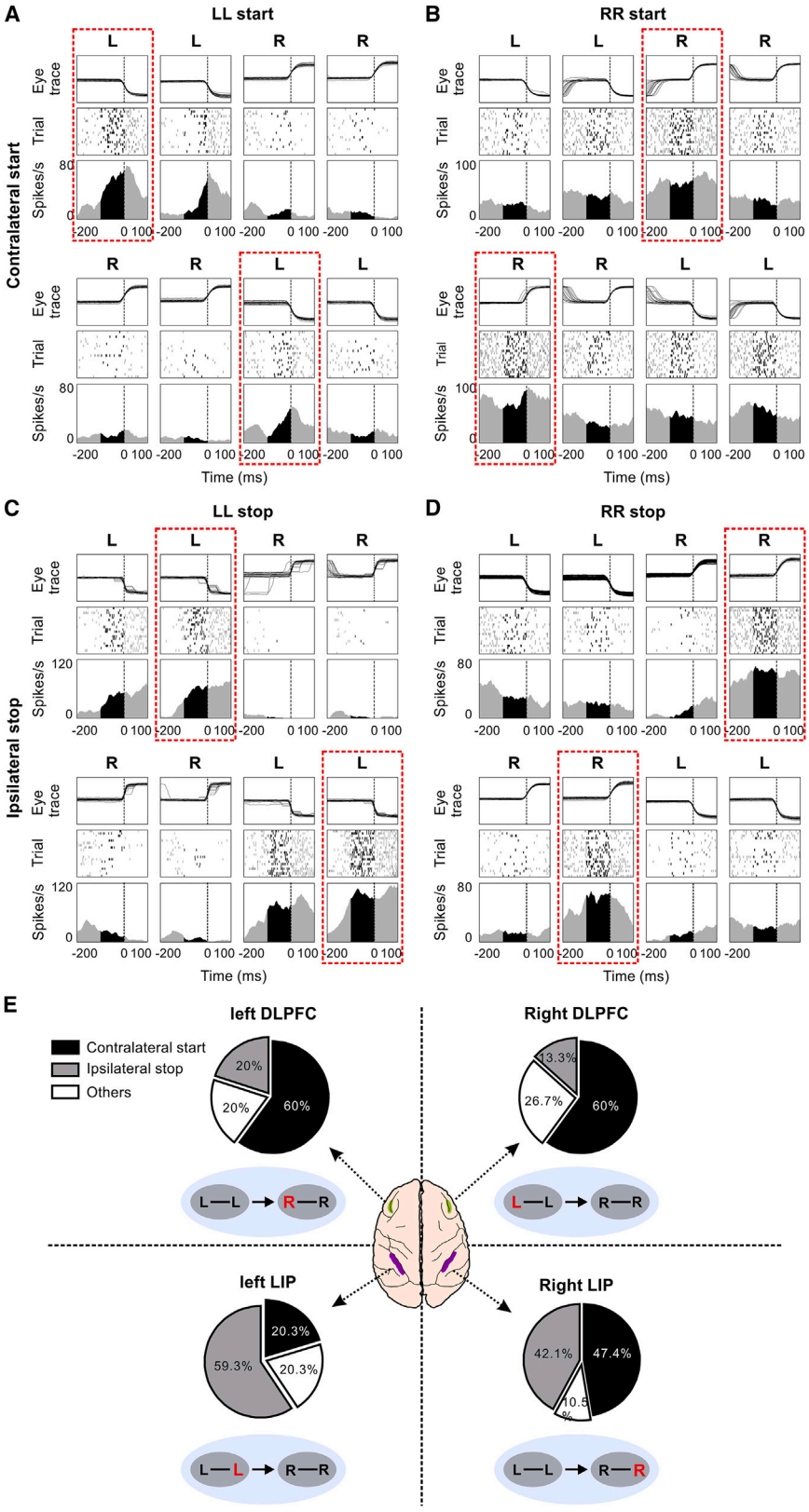

Figure 2. DLPFC mainly encodes the "start" of the contralateral subsequence while LIP primarily encodes the "stop" of the ipsilateral subsequence

(A) Example "LL start"/"Contralateral start" neuron recorded in right DLPFC.

(B) Example "RR start"/"Contralateral start" neuron recorded in left DLPFC.

(C) Example "LL stop"/"Ipsilateral stop" neuron recorded in left LIP.

(D) Example "RR stop"/"Ipsilateral stop" neuron recorded in right DLPFC. The red dashed box highlights the "start" activity of the LL subsequence (A), the "start" activity of the RR subsequence (B), the "stop" activity of the LL subsequence (C), and the "stop" activity of the RR subsequence (D), respectively.

(E) Summary of the proportion of four subtype neurons shown in (A-D).

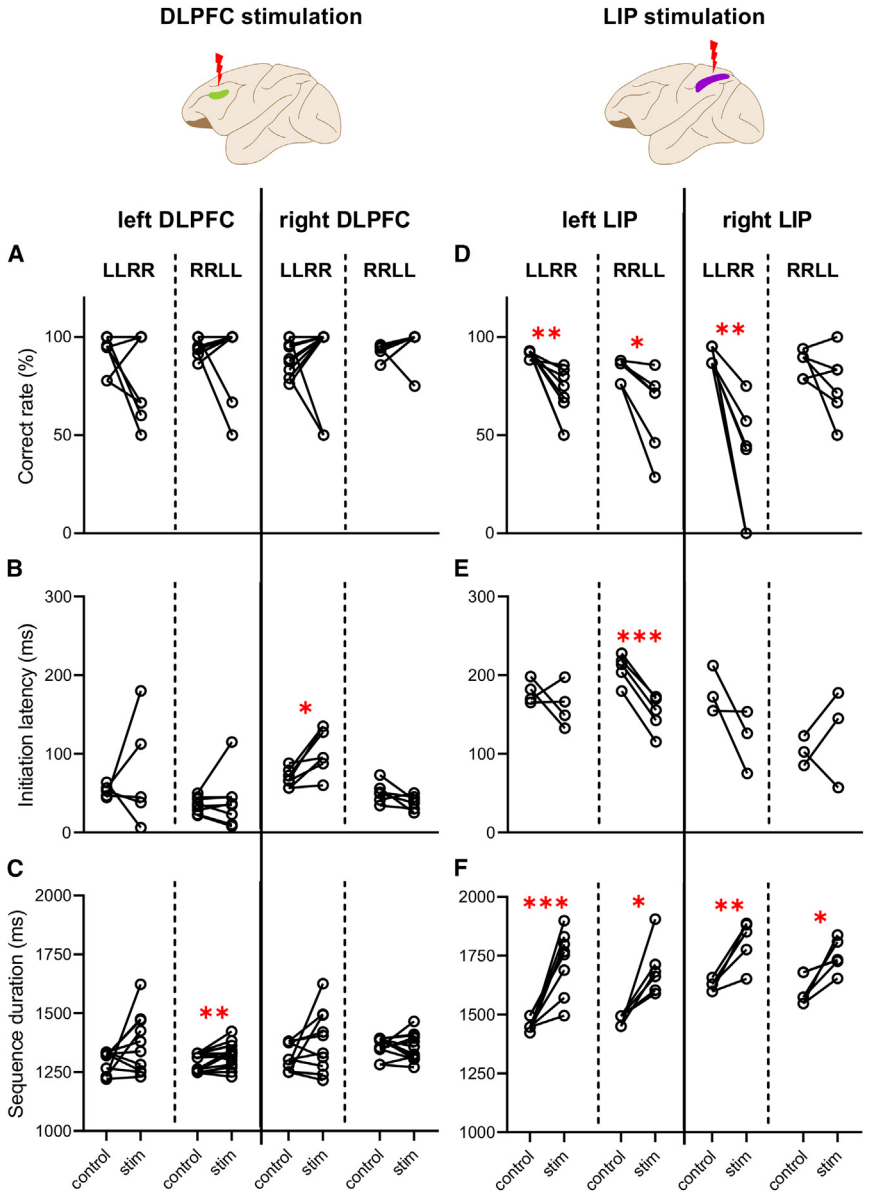

Figure 3. LIP stimulation impairs sequence execution whereas DLPFC stimulation only weakly affects sequence performance

(A–C) Change in the sequence correct rate (A), sequence initiation latency (B), and sequence duration (C) between control and DLPFC stimulation.

(D–F) Same as (A-C) for LIP stimulation. Data are calculated as mean ± SEM. A pair of "control" and "stim" points indicates a group of experiments, each group contains a total of 25∼250 trials. $^{*}p < 0.05$, $^{**}p < 0.01$, and $^{***}p < 0.001$, paired t-test. See also Figures S4 and S5.

subsequence, and the start of the contralateral subsequence, e.g., switching LL to RR subsequence in the left hemisphere.

Microstimulation of LIP impairs saccade sequence execution

To verify whether the neuronal activities in DLPFC and LIP described above causally contribute to the subsequence switch, we further applied electrical microstimulation experiments, which could influence behavior by disrupting a subset of neuronal activities. Stimulation was applied before the 1st or the 2nd saccade respectively during the sequence performance. We first analyzed the microstimulation effects on the memory-guided sequence execution, e.g., the correct rate (error trials were defined as those where the first four saccades did not match the LLRR or RRLL sequence, taking into account induced saccades), initiation latency, and sequence duration, by pooling all the datasets before 1st and 2nd saccade stimulation.

We applied microstimulation experiments in DLPFC with a current of 220 μA, as it was the maximum current that could induce saccades in LIP. Although no saccade was evoked, we noticed some interesting results: the initiation latency of the LLRR sequence was significantly increased when stimulating the right DLPFC (control vs. stim, mean ± SEM, 69.2 ± 4.4 vs. 105 ± 10.7 ms, $p = 0.0103$, paired t-test, Figure 3B), and examples of eye traces after DLPFC stimulation are presented in Figures S4A–S4D. In addition, there was a significant increase in RRLL sequence duration when stimulating the left DLPFC (control vs. stim, mean ± SEM, 1291.7 ± 9.9 vs. 1319.2 ± 13.5 ms, $p = 0.009$; paired t-test, Figure 3C). Overall, microstimulation in DLPFC weakly affected the memory-guided sequence performance. As a control, the effect of DLPFC microstimulation on the visually-guided sequence was not obvious (Figures S5A–S5C).

The current amplitude that could evoke saccades successfully in LIP ranged from 80 to 220 μA. The distribution of microstimulation-tested sites, the successful saccade-evoked sites, and data collected sites were shown in Figure S2G (see STAR Methods for details). Obvious effects were observed when stimulating LIP. Figure 3D showed that the accuracy of sequence performance was significantly decreased, except for the RRLL sequence in the condition of the right LIP stimulation (control vs. stim, mean ± SEM, left hemisphere, LLRR: 91.5 ± 0.7% vs. 70 ± 4.9%, $p = 0.0052$; RRLL: 83.6 ± 2.4% vs. 63 ± 8.7%, $p = 0.0257$; right hemisphere, LLRR: 89.5 ± 1.8% vs. 36.6 ± 12.5%, $p = 0.0084$; RRLL: 87.5 ± 2.9% vs. 75.8 ± 7%, $p = 0.1812$, paired t-test). Besides, the initiation latencies were not significantly changed, except the RRLL sequence when stimulating the left LIP (control vs. stim, mean ± SEM, left hemisphere, LLRR: 178.9 ± 7.4 vs. 161.4 ± 13.8 ms, $p = 0.4286$; RRLL: 208.7 ± 8.2 vs. 151.3 ± 10.4 ms, $p < 0.0001$; right

hemisphere, LLRR: 179.9 ± 17 vs. 118.3 ± 23 ms, p = 0.1799; RRLL: 103.7 ± 10.8 vs. 126.6 ± 36 ms, p = 0.5728, paired t-test, Figure 3E). Also, the sequence durations were significantly increased (control vs. stim, mean ± SEM, left hemisphere, LLRR: 1453.4 ± 9.9 vs. 1725.5 ± 47.6 ms, p = 0.0009; RRLL: 1479.2 ± 9.1 vs. 1692.6 ± 46.7 ms, p = 0.0103; right hemisphere, LLRR: 1622.3 ± 11.2 vs. 1809.6 ± 44 ms, p = 0.0096; RRLL: 1600 ± 25.6 vs. 1748.2 ± 26.9 ms, p = 0.0141, paired t-test, Figure 3F). Overall, LIP stimulation significantly impaired the execution of the memory-guided sequential saccades.

In contrast, the accuracy of visually-guided sequences was not significantly affected when stimulating LIP (left hemisphere, LLRR: p = 0.6344; RRLL: p = 0.9003; right hemisphere, LLRR: p = 0.1528; RRLL: p = 0.0897, paired t-test, Figure S5D), reflecting its specific effects on memory-guided sequences. Although it also significantly prolonged sequence duration (left hemisphere, LLRR: p = 0.0097; RRLL: p = 0.0137; right hemisphere, LLRR: p = 0.0141; RRLL: p = 0.0004, paired t-test, Figure S5F), the increase magnitude was smaller than that in memory-guided sequences (visually-guided vs. memory-guided, left hemisphere, LLRR: p = 0.0402; RRLL: p = 0.383; right hemisphere, LLRR: p = 0.102; RRLL: p = 0.1726, Welch's t-test).

Microstimulating LIP affects the switch between subsequences

To further examine how the electrical microstimulation on LIP altered the sequence execution, we analyzed the error trials caused by microstimulation-induced saccades. Since LIP encoded the "stop" of the ipsilateral subsequence and the "start" of the contralateral subsequence (Figure 2E), we applied stimulation within the ipsilateral subsequence (Figure 4) and contralateral subsequence (Figure 5), respectively.

In the left LIP, we hypothesized that stimulating within the LL subsequence would facilitate the switch from LL to RR subsequence, which implied that the LLRR sequence would be performed as LRR (Figure 4A). To verify this hypothesis, we analyzed the effects of microstimulation given before the 1st L and the 2nd L separately on LLRR execution (Figure 4B, top). The percentage of the induced saccade (downward) was 86.7% before the 1st L and 91.7% before the 2nd L (Figure 4B, bottom). Among the trials that successfully evoked saccades, 26.9% showed an early switch from LL to RR subsequence, and 3.8% showed a late/no switch when stimulated before the 1st L (Figure 4C). We pooled the "early switch" and "late/no switch" as an improper switch, whose percentage was significantly higher than the control (5.2%, p < 0.0001, Fisher's exact test, Figure 4D).

Similar results were obtained when stimulation was applied before the 2nd L within the LLRR sequence, with 18.2% of trials for early switch (Figure 4E). The total percentage of the improper switch (21.2%) significantly exceeded the control (5.2%, p = 0.003, Fisher's exact test, Figure 4F). A few other error trials performed after stimulation are shown in Figures S4E–S4H. These findings supported our initial hypothesis: stimulating LIP promoted the switch from the ipsilateral subsequence to the contralateral subsequence.

Notably, attempts to induce saccades through stimulation in the right LIP during the RRLL performance encountered challenges. The proportion of the evoked saccade was 5.6% before the 1st R, and 0% before the 2nd R, respectively (Figures 4G and 4H). This might be attributed to the asymmetric functions of the left and right hemispheres, as the external stimulation in the right LIP failed to disrupt the rightward saccades planned by the left LIP. Thus, further experiments regarding the performance of RRLL sequential saccades following the microstimulation did not proceed.

Later, we examined the impact of stimulation within the contralateral subsequence on sequence performance. We hypothesized that stimulating left LIP during the RRLL task might inhibit or delay the switch from RR to LL subsequence, and the RRLL sequence would be executed as RRRLL (Figure 5A). Results showed that trials exhibited successful stimulation-induced saccades (leftward) accounted for 95.2% before the 1st R, and 95.2% before the 2nd R (Figure 5B). Among these trials, improper switch in the sequence structure significantly increased if stimulation was applied before the 1st R (control vs. stim: 6.2% vs. 35.5%, p < 0.0001, Fisher's exact test, Figure 5D). They mainly characterized late/no switch from RR to LL subsequence, resulting in the RRRLL sequence (22.6%, Figure 5C). Similar outcomes emerged when stimulation was applied before the 2nd R. Significant improper switches in sequence structure occurred (control vs. stim: 6.2% vs. 40%, p = 0.0001, Fisher's exact test, Figure 5F), and the length of the RR subsequence increased, leading to a delay switch to the LL subsequence (30%, Figure 5E). Comparable phenomena were observed in the right LIP (Figures 5G–5L). These results validated our prediction that microstimulating LIP delayed the switch from the contralateral subsequence to the ipsilateral subsequence.

In sum, LIP microstimulation significantly altered the switch between subsequences, which was consistent with the neuronal representation described in Figure 2. In addition, akin to suprathreshold stimulation, subthreshold stimulation caused consistent decrease trends in sequence accuracy, along with similar sequence error types, although the reduction in sequence accuracy was not statistically significant (left hemisphere, LLRR: p = 0.5386; RRLL: p = 0.6873; right hemisphere, LLRR: p = 0.2334; RRLL: p = 0.0885, paired t-test, Figures S5G–S5M).

DLPFC inactivation increases the sequence initiation latency while LIP inactivation impairs the subsequence switch

Since microstimulation only disrupted a subset of neurons, the slight effect of DLPFC stimulation on sequence behavior might be caused by the limited effect of microstimulation on a small part of neurons. To ascertain the contributions of the whole area of DLPFC or LIP to the sequential saccades, we further performed reversible inactivation (see STAR Methods for details). Similar to Figure 3, the change in sequence correct rate, initiation latency, and duration were first analyzed after inactivation.

After muscimol injection in DLPFC, there was no significant decrease in the sequence correct rates (mean ± SEM, LLRR: −16.4 ± 8.4%, p = 0.145; RRLL: −7.4 ± 2.8%, p = 0.0816; one sample t-test, Figure 6A), and the sequence durations remained relatively unchanged (mean ± SEM, LLRR: 46.2 ± 15.8 ms, p = 0.0615; RRLL: 37.2 ± 47.3 ms, p = 0.4892, one sample t-test, Figure 6C). However, the sequence initiation latency exhibited

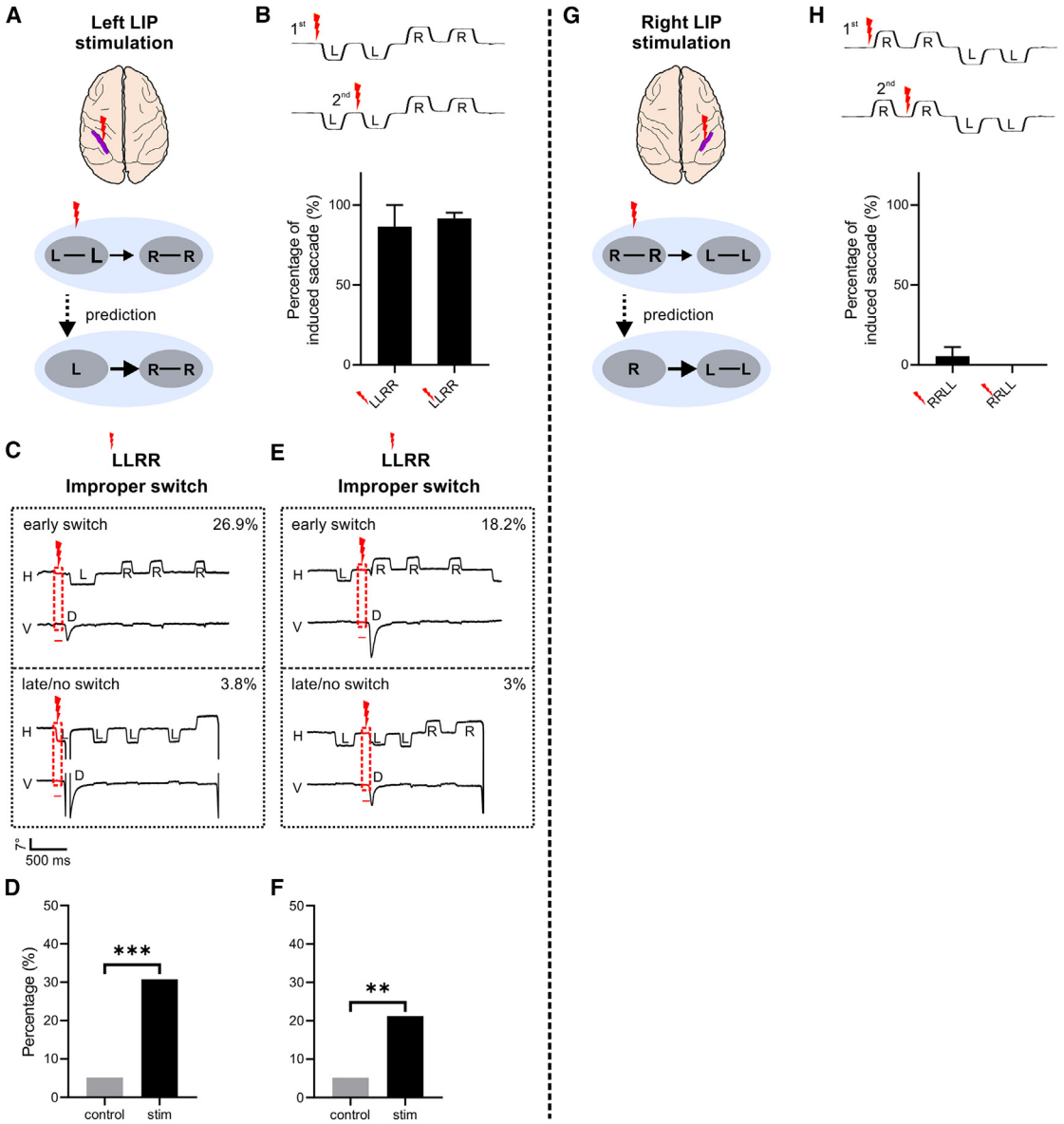

Figure 4. LIP stimulation within the ipsilateral subsequence facilitates the switch to the contralateral subsequence

(A) Schematic of prediction showing left LIP stimulation facilitates the switch from LL to RR subsequence.

(B) Design diagram for stimulation during LLRR sequence execution (top); and the percentage of the successfully induced saccades (bottom, stimulation sites: $n = 3$).

(C) Examples of eye traces showing the improper switch from LL to RR subsequence after stimulation ahead of the 1st L.

(D) Percentage of "improper switch" sequences in control (gray) and stimulus condition (black).

(E and F) Same as (C-D) for the 2nd L.

(G and H) Same as (A-B) for the right LIP. Stimulation sites: $n = 5$. Plots in (B) and (H) show mean ± SEM. A total of 578 trials were conducted for the "control" condition in (C–F), 26 trials for the "stim" condition in (C-D), and 33 trials for the "stim" condition in (E-F). $^{**}p < 0.01$, $^{***}p < 0.001$, Fisher's exact test. See also Figure S4.

significant increases for both LLRR and RRLL sequences (mean ± SEM, LLRR: 52.8 ± 1.3 ms, $p < 0.0001$; RRLL: 49.1 ± 6.6 ms, $p = 0.0051$, one sample t-test, Figures 6B and S6A–S6D), indicating that DLPFC was involved in the initiation of the overall sequence. Additional latency analysis in each saccade of the sequence as well as in single saccades following inactivation (Figures S7G and S7H) further supported the specificity of DLPFC involvement in the initiation of the learned sequence.

For LIP, a notable accuracy reduction was observed after inactivation (mean ± SEM, LLRR: −15.1 ± 4%, $p = 0.0129$; RRLL: −12.7 ± 3.2%, $p = 0.0106$, one sample t-test, Figure 6D), although the sequence initiation latency was not significantly

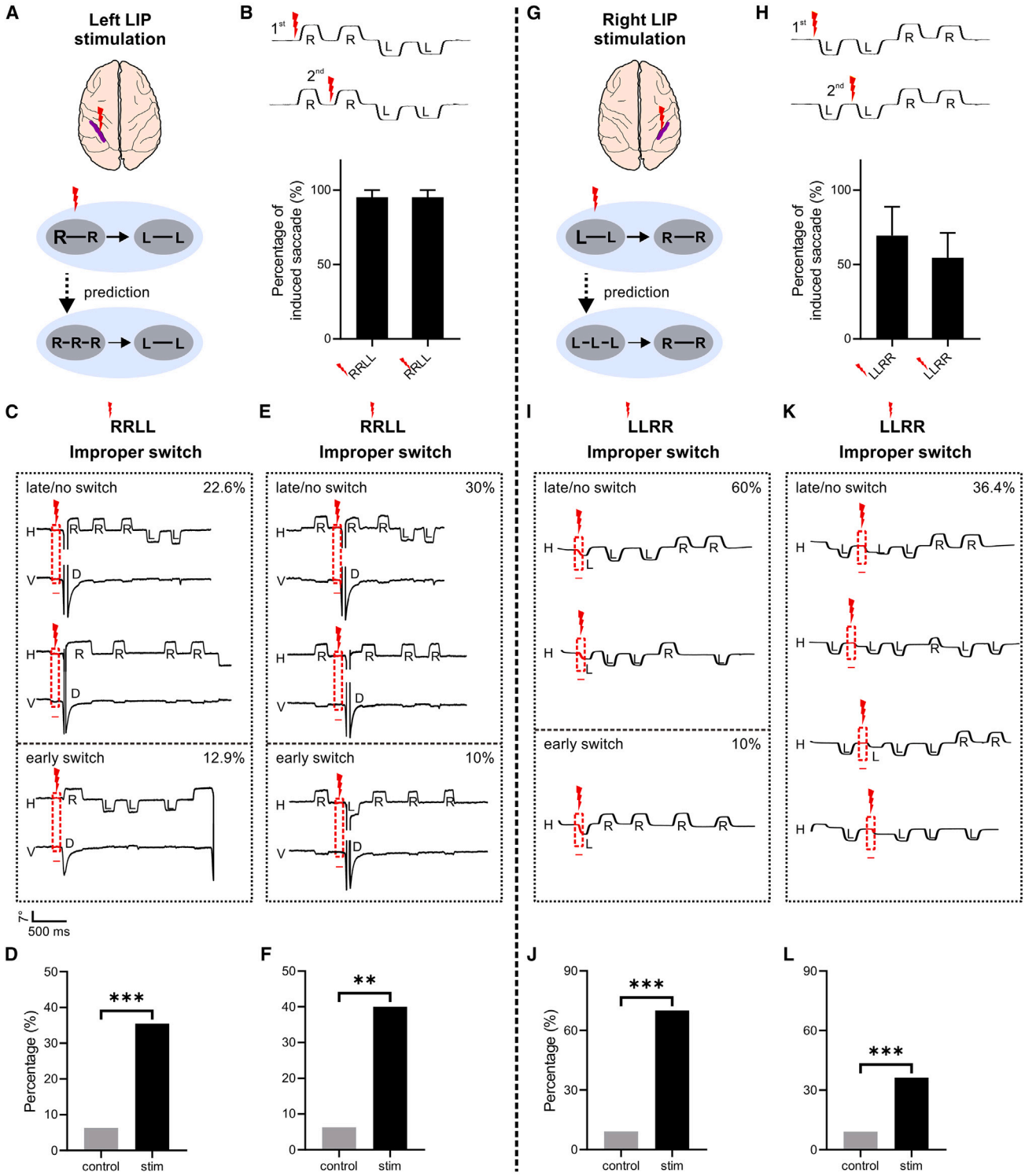

Figure 5. LIP stimulation within the contralateral subsequence delays the switch to the ipsilateral subsequence

(A) Schematic of prediction showing left LIP stimulation delays the switch from RR to LL subsequence.

(B) Design diagram for stimulation during RRLL sequence execution (top); and the percentage of the successfully induced saccade (bottom, stimulation sites: $n = 3$).

(C) Examples of eye traces showing the improper switch from RR to LL subsequence after stimulation ahead of the 1st R.

(D) Percentage of "improper switch" sequences in control (gray) and stimulus condition (black).

(legend continued on next page)

changed (mean ± SEM, LLRR: −40.5 ± 37.1 ms, p = 0.3246; RRLL: 0.5 ± 10.5 ms, p = 0.9624, one sample t-test, Figure 6E). Besides, LIP exhibited a significant increase in sequence duration after inactivation (mean ± SEM, LLRR: 137.3 ± 19.8 ms, p = 0.001; RRLL: 134.3 ± 15.8 ms, p = 0.0004; one sample t-test, Figure 6F). These data suggested that inactivating LIP directly affected sequence performance.

Then, how LIP inactivation impaired the sequence execution was further explored. Since pharmacological inactivation inhibited the neuronal activities, which might have the opposite effect compared to microstimulation, we anticipated that LIP inactivation would delay the switch from the ipsilateral subsequence to the contralateral subsequence, but promote the switch from the contralateral subsequence to the ipsilateral subsequence. In other words, after inactivating the left LIP, the switch from LL to RR subsequence would be prolonged, and the switch from RR to LL subsequence would be accelerated (Figure 7A). As expected, for the LLRR sequence, 28.8% of the trials were performed as LLL or LL, without switching to the RR subsequence. A few trials (6.8%) showed an early switch (Figure 7B). The proportion of these "improper switch" sequences was significantly increased than control (muscimol vs. control, 35.6% vs. 13.9%, $p < 0.00001$, Fisher's exact test, Figure 7C). Figures 7D and 7E illustrates the early switch (23.8%) from RR to LL subsequence after left LIP inactivation.

Similar to the left LIP, Figure 7F predicts the sequence performance after the right LIP is inactivated: the transition from RR to LL subsequence might be delayed, and the switch from LL to RR subsequence would be facilitated. The results showed that the percentage of trials with late/no switch from RR to LL subsequence was 4.3% (Figures 7G and 7H), and 4.8% exhibited an early switch from LL to RR subsequence (Figures 7I and 7J). These were consistent with our expectations, although the proportion was relatively low. Combining the results of two hemispheres, we found inactivating LIP altered the switch between subsequences. In addition, a small number of other error types of sequences executed after muscimol injection were presented in Figures S6E–S6L.

In sum, inactivation experiments also revealed different roles of DLPFC and LIP during memory-guided sequential saccades, with DLPFC involved in the initiation of the overall sequence while LIP played a role in the subsequence switch. The performance of visually-guided saccade sequences following DLPFC and LIP inactivation was barely affected, further supporting this notion (Figures S7A–S7F).

DISCUSSION

Here, we explored the roles of DLPFC and LIP in saccade sequences using a set of hierarchically organized sequential saccade tasks (left-left-right-right and right-right-left-left). The neuronal recording revealed that DLPFC and LIP differently encoded hierarchical levels of leaned saccade sequences. Microstimulating and inactivating LIP significantly affected the switch between subsequences, providing direct evidence for the causal role of LIP in the hierarchical control of the saccade sequence. Pharmacological reversible inactivation further confirmed the crucial role of DLPFC in saccade sequence initiation. The different roles of DLPFC and LIP revealed in our study proposed a foundation for understanding the cortical neuronal mechanism of the hierarchical control of the learned action sequences.

Distinct representation of sequence hierarchies in DLPFC and LIP

In the present study, we adopted a behavioral paradigm with two leftward saccades (LL) and two rightward saccades (RR) organized in LLRR and RRLL respectively. Different from previous studies with three actions in a sequence,[14,19–21] our task paradigm was easier to analyze the hierarchy organization as different sequence hierarchies were distinguished (Schematic in Figures 1C, 1E, and 1G).[5,11] We found that Sequence, Subsequence, and Element neurons coexisted in both DLPFC and LIP (Figure 1), this provided neuronal evidence for the idea that different hierarchical levels of sequence could be co-represented in a single cortical area.[16,22]

On the other hand, our results seem inconsistent with previous fMRI findings in humans, where they observed that PFC showed only sequence-level representation, and the parietal cortex exhibited an overlapped representation of chunk and sequence levels.[16] One possible reason might be the different definitions of hierarchical levels. In their research, sequence-level was defined as each sequence having its unique activate pattern, this representation might be similar to the signals encoded by the "Unclassified neurons" defined in our study. Besides, they defined the Subsequence-level representation as each subsequence/chunk having its unique encoding pattern, such classification might miss some details of the neuronal characteristics. For example, it was difficult to study the encoding features within subsequences, whereas we found that the DLPFC and LIP represented different subsequence characteristics. In addition, although the LL and RR subsequence in "Element left" neurons or the "Element right" neurons showed different firing patterns, these cells just exhibited direction preference, not containing rank information. Therefore, the discrimination for the Subsequence and Element cells in our study provided more details for the neuronal characteristics in DLPFC and LIP (Figures 1 and 2).

In our task, following each saccade to the peripheral target (L or R), a return saccade to the fixation point was required, so the monkeys executed sequences like L(R)L(R)R(L)R(L) and R(L)R(L)L(R)L(R). Our experimental paradigm was modeled after tasks previously outlined by Tanji et al., where the center-out saccades to peripheral targets rely on memory recall.[23,24] We focused solely on the 4 center-out saccades, as they shared the same starting and ending points, with the only varying factor being rank among the repeated saccades. Additionally, we classified

(E and F) Same as (C-D) for the 2nd R.

(G–L) Same as (A-F) for the right LIP. Stimulation sites: n = 3. Plots in (B) and (H) show mean ± SEM. A total of 270 trials were conducted for the "control" condition in (C-F), 31 trials for the "stim" condition in (C-D), and 20 trials for the "stim" condition in (E-F). A total of 241 trials were conducted for the "control" condition in (I–L), 10 trials for the "stim" condition in (I-J), and 11 trials for the "stim" condition in (K-L). **$p < 0.01$, ***$p < 0.001$, Fisher's exact test. See also Figure S4.

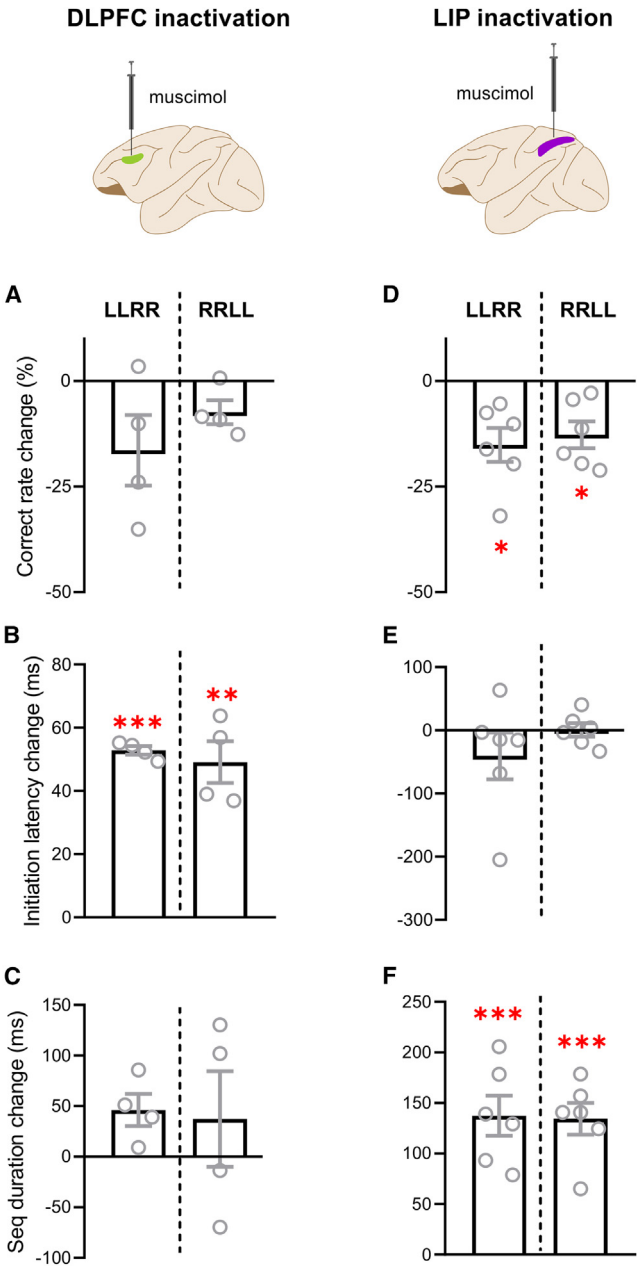

Figure 6. DLPFC inactivation increases the sequence initiation latency while LIP inactivation impairs the sequence execution

(A–C) Change in the sequence correct rate (A), sequence initiation latency (B), and sequence duration (C) between control and DLPFC inactivation.

(D–F) Change in the sequence correct rate (D), sequence initiation latency (E), and sequence duration (F) between control and LIP inactivation. Plots show mean ± SEM. $n = 4$ (A-C) or $n = 6$ (D-F) sessions of experiment, one session contains 1∼6 blocks while one block contains ∼25 trials. $^{*}p < 0.05$, $^{**}p < 0.01$, $^{***}p < 0.001$, one sample t-test. See also Figures S6 and S7.

neurons based on back saccades by using the same criteria as center-out saccades. The hierarchical representation of back saccades in LIP was consistent with that in center-out saccades, with 4.3% (16/368) for back saccade-Sequence neurons, 32.3% (119/368) for back saccade-Subsequence neurons, and 47.3% (174/368) for back saccade-Element neurons. However, in DLPFC, the classification in back saccades was different from center-out saccades (back saccade-Sequence neurons counted for 1.0% (2/194), back saccade-Subsequence neurons were 9.8% (19/194), and back saccade-Element neurons were 30.9% (60/194), this difference might be caused by the differences in the starting and ending points of the back saccades.

The role of DLPFC in the initiation of saccade sequence

In our study, DLPFC simultaneously represented several sequence hierarchies especially its representation of the "start" signals at the sequence level (Figure 1D). Such encoding characteristic was consistent with the previous finding that PFC neurons exhibited peak activities at the beginning of the sequential saccades.[13,16] Further, we applied pharmacological reversible inactivation experiments to explore the causal relationship between neuronal representation and monkey behaviors. The results showed that the "start" signals causally contributed to the sequence-level initiation (Figure 6B), and the subsequence-related activities might be just correlated with the sequential saccades.

Meanwhile, one phenomenon was noticed why does DLPFC inactivation only result in sequence delayed initiation instead of the failure to initiate? Based on previous reports, DLPFC was thought to be involved in working memory during learning a new sequence,[25] thus storing the sequence structure.[13] In the late stage of learning, the chunked structure/representation of the hierarchical sequences might be stored in the parietal cortex.[18] However, after long-term practice and the sequence can be performed skillfully (the tasks performed in our study), the role of DLPFC might no longer be important for the sequence (Figure 6). On the other hand, lesion and neuronal recording studies in monkeys suggested that DLPFC was involved in the monitoring retrieved information[26,27] or representing about rank order of the objects[20] or task progress,[28,29] implying that DLPFC might monitor whether the start of sequences is proceeding normally. Moreover, another possibility is the sequence initiation might be controlled by extra brain area instead of DLPFC. For example, pre-supplementary motor area (preSMA) might be a candidate for sequence initiation, as transcranial magnetic stimulation over human preSMA affected sequence initiation.[30,31]

The role of LIP in the transition of saccade subsequence

Microstimulation on LIP significantly altered the switch between subsequences (Figures 4 and 5), it was consistent with the neuronal representation (Figure 2E) and the subsequent inactivation effects (Figure 7). This switch role might be related to LIP's role in motor attention, as Rushworth found that parietal cortex impairment caused difficulty in shifting the motor attention from one movement to the next in a sequence.[32,33] Also, it was much more difficult for patients with parietal cortex impairment to perform heterogeneous sequences (consisting of different movements) than homogeneous sequences (consisting of repeated movements),[34,35] Rushworth thought this might be caused by the heterogeneous sequences required more frequent shifts of motor attention.[32] Therefore, this might also

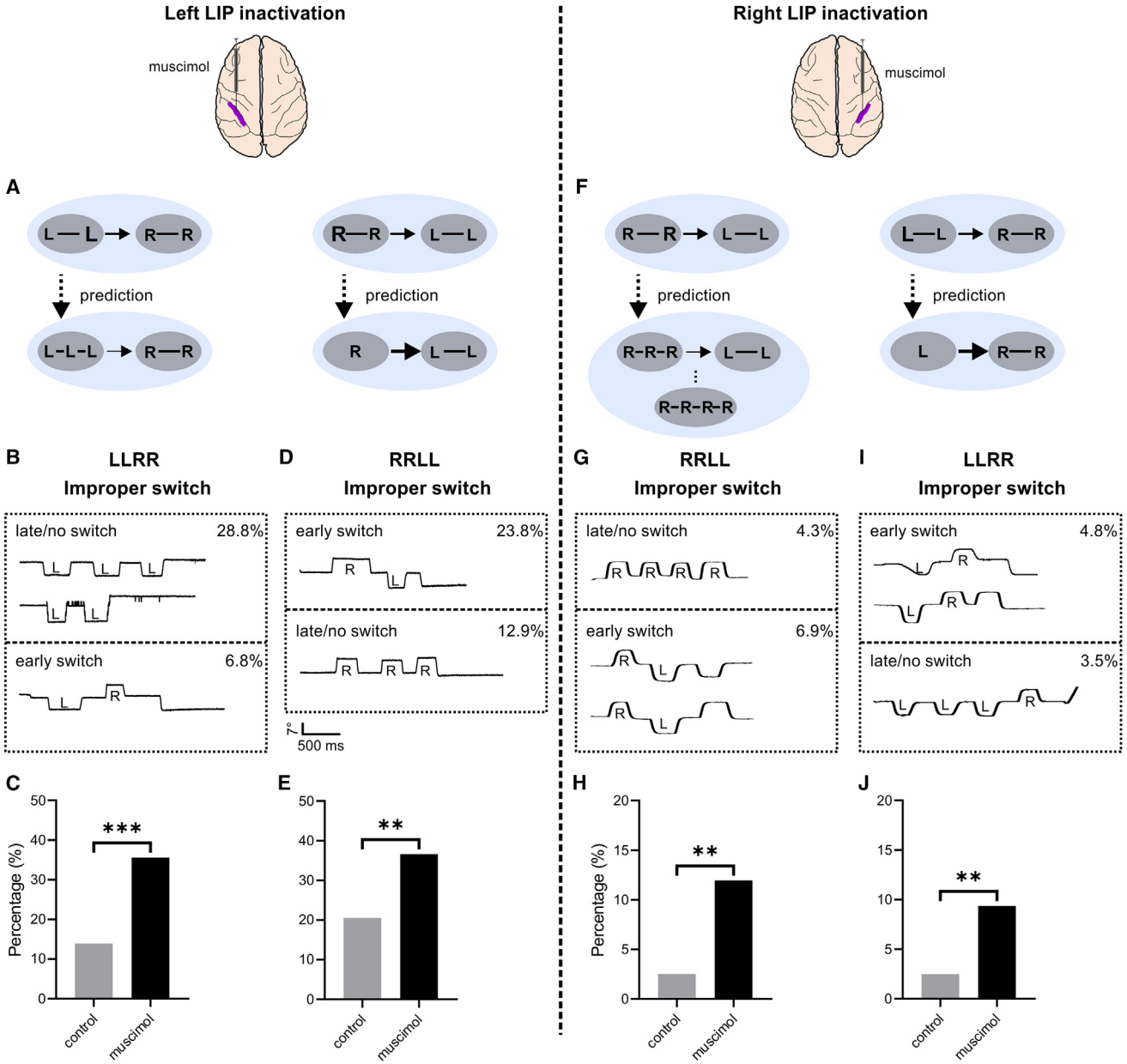

Figure 7. LIP inactivation increases "improper switch" sequences

(A) Schematic of prediction showing left LIP inactivation delays the switch from LL to RR subsequence (left) and facilitates the switch from RR to LL subsequence (right).

(B) Examples of eye traces showing the improper switch from LL to RR subsequence.

(C) Percentage of "improper switch" sequences in control (grey) and inactivation condition (black).

(D and E) Same as (B-C) for RRLL sequence.

(F–J) Same as (A–E) for the right LIP. A total of 366 trials were conducted for the "control" condition, and 146 trials for the "muscimol" condition in (B-C); 341 trials for "control", 101 trials for "muscimol" in (D-E); 241 trials for "control", 233 trials for "muscimol" in (G-H); 252 trials for "control", 227 trials for "muscimol" in (I-J). $^{**}p < 0.01$, $^{***}p < 0.001$, Fisher's exact test. See also Figure S6.

be the potential mechanism of transition role between subsequences observed in LIP.

When stimulating the right LIP, it was difficult to induce a leftward saccade, which seems inconsistent with the upcoming saccade (rightward, Figure 4H). It might be caused by the dominant role of the left LIP: the external stimulation on the right LIP failed to disrupt the plan/control for the rightward saccade of the left LIP. Asymmetric functions of the left and right parietal cortex have been reported previously: in a human task requiring mental rotation of hands, MRI showed that the range of active

area of the superior parietal lobule in the left hemisphere was larger than that of the right hemisphere[36]; Compared with the right hemisphere, the dominant role of left parietal and premotor area was more remarkable when the motor sequence was more complex[37]; Patients with ideomotor apraxia exhibited the damage of middle frontal gyrus and intraparietal sulcus (IPS) region in the left hemisphere,[38] and applying tDCS (transcranial direct current stimulation) on the left posterior parietal cortex improved their planning of skilled movements (imitating gestures).[39] Besides, hemispheric specialization was also indicated in monkeys, particularly in cognitive tasks. For instance, monkeys have demonstrated left hemisphere superiority in learning discrimination tasks involving oriented lines, such as discerning the more vertical line in a pair of straight lines[40] and discriminating whether sequentially presented stimuli are in the same or different orientations.[41] Additionally, asymmetries have been observed in visuospatial ability, with monkeys showing alterations in judging the relative position of a dot following left unilateral occipital lobectomy.[42] While these studies primarily focused on cognitive lateralization, they provide valuable insights into hemispheric specialization in monkeys. Notably, it is the first time for us to observe the asymmetric function of LIP in the sequential saccades.

Limitations of the study

Technical limitations: This study employed a conservative and robust definition of the LIP, supported by neuroimaging, histology, anatomy, and physiological evidence, to minimize the risk of stimulating areas outside LIP. However, microstimulation inherently affects a spatially confined volume of tissue, and the influence on adjacent regions, such as area 7a, cannot be completely excluded. While anatomically distinct, area 7a shares functional roles in attention and working memory, raising the possibility that it may have partially contributed to the observed effects. This limitation underscores the challenges of microstimulation studies and emphasizes the need to interpret findings within a broader anatomical and functional framework.

In addition, microstimulation elicits activity across a cluster of regions, while muscimol inactivation affects all output pathways within the targeted region, impeding the study of specific pathways and interregional interactions. The burgeoning application of optogenetics in non-human primates presents a promising avenue to address these challenges,[43] affording greater precision in modulating neuronal activity and dissecting pathway-specific contributions.

Conceptual limitations: Although our study identified brain regions associated with sequence initiation and subsequence switching, the precise area implicated in sequence termination remains elusive. While the Item-Order-Rank model suggests that the rank information originates from the posterior parietal cortices (PPC) and undergoes processing via PFC and SEF,[44] the specific role of SEF in sequence termination warrants further elucidation. Future investigations are warranted to ascertain whether SEF contributes to high-level control of sequence hierarchy and termination, potentially augmenting our understanding of the neural substrates governing sequential behavior. Moreover, exploring subcortical regions such as SC as the ultimate stage in a sequence of saccades offers further insight into the complex neural network involved in the saccadic sequence.

Furthermore, the roles of LIP and the parietal lobe in spatial information processing[45–47] and reference frame transformations[48,49] further suggest alternative interpretations of our findings. Microstimulation of LIP may disrupt spatial attention, perception, and the coordination of spatial tasks, potentially leading to difficulties in maintaining or updating spatial maps. These disruptions could impair spatial memory, eye movement coordination, and the integration of spatial and temporal information, ultimately affecting action sequences. Decisions based on spatial information may also become flawed, resulting in unexpected action sequences. While our study supports the critical role of LIP in subsequence switching, additional experiments with carefully designed behavioral controls might be needed to further dismantle these possibilities in the future.

These limitations underscore the intricate nature of investigating hierarchical organization and sequence control in the brain. Addressing these limitations will be pivotal in advancing our comprehension of the underlying neural mechanisms with greater precision and specificity.

RESOURCE AVAILABILITY

Lead contact

Further information and requests for resources and reagents should be directed to and will be fulfilled by the lead contact, Aihua Chen (ahchen@brain.ecnu.edu.cn).

Materials availability

This study did not generate new unique reagents.

Data and code availability

- Data have been deposited at Zenodo and are publicly available as of the date of publication. DOIs are listed in the key resources table.
- All original code has been deposited at Zenodo and is publicly available as of the date of publication. DOIs are listed in the key resources table.
- Any additional information required to reanalyze the data reported in this paper is available from the lead contact upon request.

ACKNOWLEDGMENTS

This work was supported by grants from the “STI2030-major projects” (No.2021ZD0202600), the National Basic Research Program of China (32171034, 31871079), the Shanghai Municipal Science and Technology Major Project (2021SHZDZX, 2018SHZDZX05) to A.C., and ECNU startup fund to X.J. We are grateful to Minhu Chen for computer programming. We also thank BioRender for our graphical abstract preparation.

AUTHOR CONTRIBUTIONS

Conceptualization, A.C., X.J., B.S., and Q.W.; methodology, A.C., X.J., Q.W., and B.S.; software, A.C., J.J., B.S., and Q.W.; validation, Q.W., B.S., and J.J.; formal analysis, Q.W. and B.S.; investigation, J.J., Q.W., B.S., J.H., and H.L.; resources, A.C., J.J., Q.W., B.S., H.L., and J.H.; data curation, Q.W.; writing – original draft, Q.W. and B.S.; writing – review and editing, A.C., X.J., Q.W., and B.S.; visualization, B.S., and Q.W.; supervision, A.C. and X.J.; project administration, A.C.; funding acquisition, A.C.

DECLARATION OF INTERESTS

The authors declare no competing interests.

STAR★METHODS

Detailed methods are provided in the online version of this paper and include the following:

- KEY RESOURCES TABLE
- EXPERIMENTAL MODEL AND STUDY PARTICIPANT DETAILS
- METHOD DETAILS
  - Surgery
  - MRI scanning
  - Memory-guided saccade (MGS) task
  - Sequential saccade tasks
  - Electrophysiological recording
  - Electrical microstimulation
  - Pharmacological reversible inactivation
  - Cell classification
- QUANTIFICATION AND STATISTICAL ANALYSIS

SUPPLEMENTAL INFORMATION

Supplemental information can be found online at https://doi.org/10.1016/j.isci.2024.111694.

Received: December 15, 2023
Revised: December 6, 2024
Accepted: December 23, 2024
Published: December 26, 2024

REFERENCES

1. Lashley, K.S. (1951). The Problem of Serial Order in Behavior. In Cerebral mechanisms in behavior; the Hixon Symposium (Wiley), pp. 112–146.
2. Miller, G.A. (1956). The magical number seven, plus or minus two: Some limits on our capacity for processing information. Psychol. Rev. *63*, 81–97. https://doi.org/10.1037/h0043158.
3. Gallistel, C.R. (1982). The Organization of Action: A New Synthesis (Psychology Press). https://doi.org/10.4324/9780203780794.
4. Rosenbaum, D.A., Cohen, R.G., Jax, S.A., Weiss, D.J., and van der Wel, R. (2007). The problem of serial order in behavior: Lashley's legacy. Hum. Mov. Sci. *26*, 525–554. https://doi.org/10.1016/j.humov.2007.04.001.
5. Geddes, C.E., Li, H., and Jin, X. (2018). Optogenetic Editing Reveals the Hierarchical Organization of Learned Action Sequences. Cell *174*, 32–43.e15. https://doi.org/10.1016/j.cell.2018.06.012.
6. Sparks, D.L. (2002). The brainstem control of saccadic eye movements. Nat. Rev. Neurosci. *3*, 952–964. https://doi.org/10.1038/nrn986.
7. Munoz, D.P., and Everling, S. (2004). Look away: the anti-saccade task and the voluntary control of eye movement. Nat. Rev. Neurosci. *5*, 218–228. https://doi.org/10.1038/nrn1345.
8. Pierrot-Deseilligny, C., Milea, D., and Müri, R.M. (2004). Eye movement control by the cerebral cortex. Curr. Opin. Neurol. *17*, 17–25. https://doi.org/10.1097/00019052-200402000-00005.
9. Phillips, A.N., and Segraves, M.A. (2010). Predictive Activity in Macaque Frontal Eye Field Neurons During Natural Scene Searching. J. Neurophysiol. *103*, 1238–1252. https://doi.org/10.1152/jn.00776.2009.
10. Basu, D., and Murthy, A. (2020). Parallel programming of saccades in the macaque frontal eye field: are sequential motor plans coactivated? J. Neurophysiol. *123*, 107–119. https://doi.org/10.1152/jn.00545.2018.
11. Jia, J., Puyang, Z., Wang, Q., Jin, X., and Chen, A. (2021). Dynamic encoding of saccade sequences in primate frontal eye field. J. Physiol. *599*, 5061–5084. https://doi.org/10.1113/JP282094.
12. Pierrot-Deseilligny, C., Müri, R.M., Ploner, C.J., Gaymard, B., and Rivaud-Péchoux, S. (2003). Cortical control of ocular saccades in humans: a model for motricity. In Progress in Brain Research Neural Control of Space Coding and Action Production (Elsevier), pp. 3–17. https://doi.org/10.1016/S0079-6123(03)42003-7.
13. Fujii, N., and Graybiel, A.M. (2003). Representation of Action Sequence Boundaries by Macaque Prefrontal Cortical Neurons. Science *301*, 1246–1249. https://doi.org/10.1126/science.1086872.
14. Ninokura, Y., Mushiake, H., and Tanji, J. (2003). Representation of the temporal order of visual objects in the primate lateral prefrontal cortex. J. Neurophysiol. *89*, 2868–2873. https://doi.org/10.1152/jn.00647.2002.
15. Shima, K., Isoda, M., Mushiake, H., and Tanji, J. (2007). Categorization of behavioural sequences in the prefrontal cortex. Nature *445*, 315–318. https://doi.org/10.1038/nature05470.
16. Yokoi, A., and Diedrichsen, J. (2019). Neural Organization of Hierarchical Motor Sequence Representations in the Human Neocortex. Neuron *103*, 1178–1190.e7. https://doi.org/10.1016/j.neuron.2019.06.017.
17. Sadato, N., Campbell, G., Ibáñez, V., Deiber, M., and Hallett, M. (1996). Complexity affects regional cerebral blood flow change during sequential finger movements. J. Neurosci. *16*, 2691–2700. https://doi.org/10.1523/JNEUROSCI.16-08-02691.1996.
18. Sakai, K., Kitaguchi, K., and Hikosaka, O. (2003). Chunking during human visuomotor sequence learning. Exp. Brain Res. *152*, 229–242. https://doi.org/10.1007/s00221-003-1548-8.
19. Barone, P., and Joseph, J.-P. (1989). Prefrontal cortex and spatial sequencing in macaque monkey. Exp. Brain Res. *78*, 447–464. https://doi.org/10.1007/BF00230234.
20. Ninokura, Y., Mushiake, H., and Tanji, J. (2004). Integration of Temporal Order and Object Information in the Monkey Lateral Prefrontal Cortex. J. Neurophysiol. *91*, 555–560. https://doi.org/10.1152/jn.00694.2003.
21. Berdyyeva, T.K., and Olson, C.R. (2010). Rank Signals in Four Areas of Macaque Frontal Cortex During Selection of Actions and Objects in Serial Order. J. Neurophysiol. *104*, 141–159. https://doi.org/10.1152/jn.00639.2009.
22. Botvinick, M.M. (2007). Multilevel structure in behaviour and in the brain: a model of Fuster's hierarchy. Philos. Trans. R. Soc. Lond. B Biol. Sci. *362*, 1615–1626. https://doi.org/10.1098/rstb.2007.2056.
23. Isoda, M., and Tanji, J. (2002). Cellular Activity in the Supplementary Eye Field During Sequential Performance of Multiple Saccades. J. Neurophysiol. *88*, 3541–3545. https://doi.org/10.1152/jn.00299.2002.
24. Isoda, M., and Tanji, J. (2003). Contrasting Neuronal Activity in the Supplementary and Frontal Eye Fields During Temporal Organization of Multiple Saccades. J. Neurophysiol. *90*, 3054–3065. https://doi.org/10.1152/jn.00367.2003.
25. Hikosaka, O., Nakahara, H., Rand, M.K., Sakai, K., Lu, X., Nakamura, K., Miyachi, S., and Doya, K. (1999). Parallel neural networks for learning sequential procedures. Trends Neurosci. *22*, 464–471. https://doi.org/10.1016/S0166-2236(99)01439-3.
26. Petrides, M. (1991). Monitoring of selections of visual stimuli and the primate frontal cortex. Proc. Biol. Sci. *246*, 293–298. https://doi.org/10.1098/rspb.1991.0157.
27. Petrides, M. (1991). Functional specialization within the dorsolateral frontal cortex for serial order memory. Proc. Biol. Sci. *246*, 299–306. https://doi.org/10.1098/rspb.1991.0158.
28. Hasegawa, R.P., Blitz, A.M., and Goldberg, M.E. (2004). Neurons in Monkey Prefrontal Cortex Whose Activity Tracks the Progress of a Three-Step Self-Ordered Task. J. Neurophysiol. *92*, 1524–1535. https://doi.org/10.1152/jn.01110.2003.
29. Hoshi, E., and Tanji, J. (2004). Area-Selective Neuronal Activity in the Dorsolateral Prefrontal Cortex for Information Retrieval and Action Planning. J. Neurophysiol. *91*, 2707–2722. https://doi.org/10.1152/jn.00904.2003.
30. Kennerley, S.W., Sakai, K., and Rushworth, M.F.S. (2004). Organization of Action Sequences and the Role of the Pre-SMA. J. Neurophysiol. *91*, 978–993. https://doi.org/10.1152/jn.00651.2003.

31. Muessgens, D., Thirugnanasambandam, N., Shitara, H., Popa, T., and Hallett, M. (2016). Dissociable roles of preSMA in motor sequence chunking and hand switching—a TMS study. J. Neurophysiol. *116*, 2637–2646. https://doi.org/10.1152/jn.00565.2016.

32. Rushworth, M.F., Nixon, P.D., Renowden, S., Wade, D.T., and Passingham, R.E. (1997). The left parietal cortex and motor attention. Neuropsychologia *35*, 1261–1273. https://doi.org/10.1016/S0028-3932(97)00050-X.

33. Rushworth, M.F.S., Johansen-Berg, H., Göbel, S.M., and Devlin, J.T. (2003). The left parietal and premotor cortices: motor attention and selection. Neuroimage *20*, S89–S100. https://doi.org/10.1016/j.neuroimage.2003.09.011.

34. Harrington, D.L., and Haaland, K.Y. (1991). Hemispheric specialization for motor sequencing: abnormalities in levels of programming. Neuropsychologia *29*, 147–163. https://doi.org/10.1016/0028-3932(91)90017-3.

35. Harrington, D.L., and Haaland, K.Y. (1992). Motor sequencing with left hemisphere damage. Are some cognitive deficits specific to limb apraxia? Brain *115*, 857–874. https://doi.org/10.1093/brain/115.3.857.

36. Bonda, E., Petrides, M., Frey, S., and Evans, A. (1995). Neural correlates of mental transformations of the body-in-space. Proc. Natl. Acad. Sci. USA *92*, 11180–11184. https://doi.org/10.1073/pnas.92.24.11180.

37. Haaland, K.Y., Elsinger, C.L., Mayer, A.R., Durgerian, S., and Rao, S.M. (2004). Motor Sequence Complexity and Performing Hand Produce Differential Patterns of Hemispheric Lateralization. J. Cogn. Neurosci. *16*, 621–636. https://doi.org/10.1162/089892904323057344.

38. Haaland, K.Y., Harrington, D.L., and Knight, R.T. (2000). Neural representations of skilled movement. Brain *123*, 2306–2313. https://doi.org/10.1093/brain/123.11.2306.

39. Bolognini, N., Convento, S., Banco, E., Mattioli, F., Tesio, L., and Vallar, G. (2015). Improving ideomotor limb apraxia by electrical stimulation of the left posterior parietal cortex. Brain *138*, 428–439. https://doi.org/10.1093/brain/awu343.

40. Hamilton, C.R., and Vermeire, B.A. (1988). Complementary Hemispheric Specialization in Monkeys. Science *242*, 1691–1694. https://doi.org/10.1126/science.3201258.

41. Vogels, R., Saunders, R.C., and Orban, G.A. (1994). Hemispheric lateralization in rhesus monkeys can be task-dependent. Neuropsychologia *32*, 425–438. https://doi.org/10.1016/0028-3932(94)90088-4.

42. Jason, G.W., Cowey, A., and Weiskrantz, L. (1984). Hemispheric asymmetry for a visuo-spatial task in monkeys. Neuropsychologia *22*, 777–784. https://doi.org/10.1016/0028-3932(84)90102-7.

43. Mendoza-Halliday, D., Xu, H., Azevedo, F.A.C., and Desimone, R. (2024). Dissociable neuronal substrates of visual feature attention and working memory. Neuron *112*, 850–863.e6. https://doi.org/10.1016/j.neuron.2023.12.007.

44. Dickman, J.D., and Angelaki, D.E. (2002). Vestibular Convergence Patterns in Vestibular Nuclei Neurons of Alert Primates. J. Neurophysiol. *88*, 3518–3533. https://doi.org/10.1152/jn.00518.2002.

45. Andersen, R.A., and Buneo, C.A. (2002). Intentional maps in posterior parietal cortex. Annu. Rev. Neurosci. *25*, 189–220. https://doi.org/10.1146/annurev.neuro.25.112701.142922.

46. Bisley, J.W., and Goldberg, M.E. (2003). Neuronal Activity in the Lateral Intraparietal Area and Spatial Attention. Science *299*, 81–86. https://doi.org/10.1126/science.1077395.

47. Colby, C.L., and Goldberg, M.E. (1999). SPACE AND ATTENTION IN PARIETAL CORTEX. Annu. Rev. Neurosci. *22*, 319–349. https://doi.org/10.1146/annurev.neuro.22.1.319.

48. Caruso, V.C., Mohl, J.T., Glynn, C., Lee, J., Willett, S.M., Zaman, A., Ebihara, A.F., Estrada, R., Freiwald, W.A., Tokdar, S.T., and Groh, J.M. (2018). Single neurons may encode simultaneous stimuli by switching between activity patterns. Nat. Commun. *9*, 2715. https://doi.org/10.1038/s41467-018-05121-8.

49. Caruso, V.C., Pages, D.S., Sommer, M.A., and Groh, J.M. (2021). Compensating for a shifting world: evolving reference frames of visual and auditory signals across three multimodal brain areas. J. Neurophysiol. *126*, 82–94. https://doi.org/10.1152/jn.00385.2020.

50. Gu, Y., Watkins, P.V., Angelaki, D.E., and DeAngelis, G.C. (2006). Visual and Nonvisual Contributions to Three-Dimensional Heading Selectivity in the Medial Superior Temporal Area. J. Neurosci. *26*, 73–85. https://doi.org/10.1523/JNEUROSCI.2356-05.2006.

51. Barash, S., Bracewell, R.M., Fogassi, L., Gnadt, J.W., and Andersen, R.A. (1991). Saccade-related activity in the lateral intraparietal area. I. Temporal properties; comparison with area 7a. J. Neurophysiol. *66*, 1095–1108. https://doi.org/10.1152/jn.1991.66.3.1095.

52. Barash, S., Bracewell, R.M., Fogassi, L., Gnadt, J.W., and Andersen, R.A. (1991). Saccade-related activity in the lateral intraparietal area. II. Spatial properties. J. Neurophysiol. *66*, 1109–1124. https://doi.org/10.1152/jn.1991.66.3.1109.

53. Chen, L.L., Goffart, L., and Sparks, D.L. (2001). A simple method for constructing microinjectrodes for reversible inactivation in behaving monkeys. J. Neurosci. Methods *107*, 81–85. https://doi.org/10.1016/S0165-0270(01)00354-5.

54. Chen, A., Gu, Y., Liu, S., DeAngelis, G.C., and Angelaki, D.E. (2016). Evidence for a Causal Contribution of Macaque Vestibular, But Not Intraparietal, Cortex to Heading Perception. J. Neurosci. *36*, 3789–3798. https://doi.org/10.1523/JNEUROSCI.2485-15.2016.

55. Chowdhury, S.A., and DeAngelis, G.C. (2008). Fine Discrimination Training Alters the Causal Contribution of Macaque Area MT to Depth Perception. Neuron *60*, 367–377. https://doi.org/10.1016/j.neuron.2008.08.023.

56. Gu, Y., DeAngelis, G.C., and Angelaki, D.E. (2012). Causal Links between Dorsal Medial Superior Temporal Area Neurons and Multisensory Heading Perception. J. Neurosci. *32*, 2299–2313. https://doi.org/10.1523/JNEUROSCI.5154-11.2012.

57. Arikan, R., Blake, N.M.J., Erinjeri, J.P., Woolsey, T.A., Giraud, L., and Highstein, S.M. (2002). A method to measure the effective spread of focally injected muscimol into the central nervous system with electrophysiology and light microscopy. J. Neurosci. Methods *118*, 51–57. https://doi.org/10.1016/S0165-0270(02)00143-7.

STAR★METHODS

KEY RESOURCES TABLE

REAGENT or RESOURCE	SOURCE	IDENTIFIER
Chemicals, peptides, and recombinant proteins		
Muscimol	Sigma	M1523-5MG
Deposited data		
Raw data	This study	Zenodo Data: https://doi.org/10.5281/zenodo.14540231
Experimental models: Organisms/strains		
Rhesus macaques	China	N/A
Software and algorithms		
Code for analysis	This study	Zenodo Data: https://doi.org/10.5281/zenodo.14540231
Spike2	Cambridge Electronic Design Limited	Version V8
MATLAB	MathWorks	Version 2016b
GraphPad Prism 8	GraphPad	Version 8.0.1
Origin Pro	OriginLab	Version 2017C

EXPERIMENTAL MODEL AND STUDY PARTICIPANT DETAILS

Five adult male rhesus macaques (*Macaca mulatta*, C, E, F, I, and M, 8∼12 years, weighing 7.5 kg, 12 kg, 8 kg, 8 kg, and 10.5 kg, respectively) were trained and cared for in the East China Normal University Primate Center. Since the consistent sex among animals, results would not be affected by sex factor. All monkeys were solo-housed in a simulated 12:12 (7:00 a.m. & 7:00 p.m.) diurnal cycle with a temperature of 22∼26°C and humidity of 40∼70%, and their weights were monitored twice each week. During recording periods, animals would follow a controlled water intake, and a fruit reward was offered after recording. All experiments were approved by the Institutional Animal Care and Use Committee at East China Normal University (IACUC protocol number: mon20180302).

METHOD DETAILS

Surgery

Animal surgery contains head restraint and eye coil implantation.[11,44,50] Animals were intramuscular (IM) injected with atropine (0.05 mg/kg) and ketamine (15 mg/kg) first and followed by inhalation anesthesia of isoflurane (1∼3%) in surgery. Prophylactic antibiotics (Baytril, 5 mg/kg, IM) and analgesics (tolfedine, 4 mg/kg, IM) were used once and twice a day respectively to prevent post-surgery infection and pain. The recovery period of head restraint and eye coil implantation was 3∼6 months and 1∼2 weeks, respectively.

Head-restraint implantation: In surgery, the head of the monkey was fixed in a stereotaxic holder and its hair was removed. After the scalp was sterilized with medical iodophor, the skin over the head restraint position was incised along the sagittal suture, and soft tissues were removed to expose the skull. Then, a set of plastic head-restraint rings (outer diameter: 6 cm) was fixed to the six titanium screws threaded into the skull. Finally, dental acrylic was used to immobilize and seal the plastic rings, and a matching cap was placed in non-recording time to keep the inside of the implant clean. The ring was placed in the horizontal plane with the center at anteroposterior (AP) 1.4 cm for monkey C, AP 1.8 cm for monkey I, AP 0.8 cm for monkey E, AP 0.8 cm for monkey F, AP 0 for monkey M. During experiments, the monkey's head was firmly anchored to the apparatus by attaching a custom fitting collar to the plastic ring.

Once the monkeys were sufficiently trained, a customized recording grid constructed of plastic (Delrin) was fitted inside the ring and stereotaxically secured to the skull using dental acrylic. The grid was placed in the horizontal plane about 1∼3 cm to the surface of the skull. The grid contained staggered rows of holes (spaced 0.8 mm apart) that allowed the insertion of microelectrodes vertically into the brain via transdural guide tubes that were passed through a small burr hole in the skull.[44] The grid extended from the sagittal suture to the area overlying LIP/DLPFC bilaterally.

Eye coil implantation: A circular part of the conjunctiva around the cornea was dissected away first. Then, a suitable, sterilized eye coil was implanted beneath the conjunctiva and fixed on the sclera with insoluble sutures (Ningbo Microscopic Instrument Factory, Zhejiang, China). The lead wires of the eye coil left the orbit through the conjunctiva and were guided by a surgical needle under the muscle and skin to the internal of the head-restraint ring. Finally, a connector plug was soldered to the lead wires and half-buried in

the head restraint ring with dental acrylic. During the surgery, oxybuprocaine hydrochloride eye drops (4 mg/mL, Santen Pharmaceutical Co. Ltd, Osaka, Japan) were used to retard the swelling of the conjunctiva periodically.

MRI scanning

To precisely identify the brain regions, each monkey was implemented structural MRI scanning (Siemens Medical Systems Ltd, Magnetom Prisma 3.0T, Erlangen, Germany) at least twice times. The first time was before the head-restraint implantation and the second time was before the electrophysiological recording.

On the day of MRI scanning, monkeys were anesthetized by intramuscular injection of atropine (0.05 mg/kg) and ketamine (15 mg/kg), then transported to the Imaging Center at East China Normal University. Before scanning, the monkey's head was fixed in an MRI-compatible stereotaxic frame (DAVID KOPF INSTRUMENTS, Model 1430M MRI Stereotaxic Instrument, Tujunga, CA, USA), and a head coil for non-human primates was placed over the appropriate location of the head. Specifically in the second time scanning, small cannulae filled with a positive contrast agent (vitamin E) were inserted into the recording grid to confirm recording sites with the MRI volume. Then MRI scanning was performed using a high-resolution sagittal MPRAGE sequence (0.6 mm × 0.6 mm × 0.6 mm voxels) and the overall scanning procedure was about 15 min.

Memory-guided saccade (MGS) task

Firstly, the monkey was required to gaze at the white fixation point (0.3°, circular) within a 5 × 5° window for 500 ms. Then a red target point (1°, circular) appeared in one of the eight possible directions (0°, 45°, 90°, 135°, 180°, 225°, 270°, 315°, 360°), 7° away from the fixation point, and disappeared 200 ms later, during which the monkey keep gazing the fixation point. After the disappearance of the target point, the monkey was required to make a rapid eye movement to the target position within 500 ms after a delay time of 800∼1100 ms. The target would reappear if the monkey reached the target position, and a reward was delivered after maintaining the target position for 350 ms within 5 ° × 5 ° window. MGS task was used to identify whether the recording neurons were in LIP, which would exhibit persistent activity during the memory period.[51,52]

Sequential saccade tasks

Monkeys were required to learn two sequential saccade tasks, Left-Left-Right-Right (LLRR) and Right-Right-Left-Left (RRLL). For each task, they were first taught this task by visually-guided sequential saccade tasks, then learned memory-guided sequential saccade tasks. Details were as follows.

Visually-guided sequential saccades task: For the LLRR sequential saccade task (Figure 1A, top red), a white fixation point (0.3°, circular) in the center and two red targets (0.3°, circular) on either side (7° left or right relative to the fixation point, respectively) were presented on the screen. The monkey was first required to fix on the white fixation point for 200 ms within the 5 ° × 5 ° window. Then, the fixation point disappeared, meanwhile, the red target point to the left of the center changed to white, prompting the monkey to saccade to the left target (within the window of 5 ° × 5 ° centered at 7°relative to the fixation point) within 2000 ms. Then the central fixation point appeared again, meanwhile, the left white target point changed to red again, and the monkey made a saccade back to the central fixation point within 1000ms, which indicates the first left saccade of the sequence was completed. The remaining left, right, and right saccades in the sequence were then performed similarly, and the reward was delivered until the LLRR was finished.

Memory-guided sequential saccades task: The difference between the memory-guided sequential saccades and visually-guided sequential saccade task was that when the fixation point disappeared, both of the two target points kept red, and the monkey made a saccade to the left from previous memories. Then the central fixation point appeared again, prompting the monkey to saccade back to the center. Similarly, the monkey continued to complete the remaining three saccades. The reward was delivered until the memory-guided LLRR sequence was finished.

The RRLL sequential saccade task was learned in the same way after the monkeys had learned the LLRR saccade sequence. In short, the completion of the sequence has no time limit and is self-paced. In the subsequent experiments, the visually-guided and memory-guided sequence tasks appeared randomly in each block (50 trials total for electrophysiological recording, 100∼200 trials for microstimulation experiment) with a ratio of 1:1, and the data on memory-guided saccade sequences were used for analysis.

Electrophysiological recording

When the correct rate of each sequential saccade task exceeded 75%, we started single-unit recordings in the area of DLPFC and LIP (Figure S1). The recording tungsten microelectrodes (Frederick Haer Company; impedance, 1∼2 MΩ at 1 kHz) were inserted into the cortex by a hydraulic microdrive (Frederick Haer Company, Bowdoin, ME, USA) through a guide tube. The guide tube was limited by interleaved holes in the recording grid installed in the head-restraint rings. The diameter of the recording grid hole was 0.5 mm and the center distance between each hole was 0.8 mm. Neural signals were recorded and sorted online using AlphaLab SnR (AlphaOmega Instruments, Nazareth Illit, Israel) or sorted offline separately using the software Spike2 V8 (Cambridge Electronic Design Limited, Cambridge, UK).

Electrical microstimulation

To further explore the functional causal association between brain areas and sequential saccades, electrical microstimulation was applied on LIP and DLPFC. According to the trend of gray matter mapped by electrophysiology and the characteristic response to the

MGS task of the LIP neuron, we mapped the LIP range and performed microstimulation tests spaced a grid hole to find the sites that could be triggered saccades. Electrodes were inserted into the cortex, and stimulation was applied at intervals of 300∼500 μm to observe a saccadic response. Then, current ranging from 80∼250 μA (with a frequency of 200 Hz, a pulse width of 200 μs, and a pulse interval of 100 μs, for a duration of 100 ms) was applied on these sites, which magnitude depended on the threshold of inducing saccades. In each site, several blocks of trials (each block consisted of 100∼200 trials) for each sequential saccade task were performed, of which 20% were delivered by electric microstimulation and the others as controls. Microstimulation was given at different saccade locations of the performing sequential saccade to study whether the effect on disrupting different locations was different. In the left LIP, a total of 41 penetrations were tested to observe whether saccade could be induced by microstimulation, of which 15 penetrations were able to induce saccade with the threshold current of 80∼220 μA, most of them were induced with downward saccades. We then collected behavior data from 4 penetrations within them, since they could be stably evoked saccades during a total of 200∼500 trials with relatively lower current compared to other penetrations. In the right LIP, 4 of 51 tested penetrations were able to induce saccades with the threshold current of 200∼220 μA, and behavior data were collected within 2 of 3 penetrations, of which the induced saccades were leftward. The distribution of these penetrations is presented in Figure S2G. Microstimulation did not trigger saccades in DLPFC, for comparison, the max current (220 μA) in LIP experiment was used in further DLPFC experiments.

It is necessary to note that the reward would be delivered after 4 saccades made into the target window, whether the saccades were triggered by stimulation or made by the monkey itself. So, when stimulating the last two saccades of the sequence, it was difficult to distinguish the saccade performance after stimulation was caused by stimulation or by reward. Therefore, microstimulation was randomly given on one of the first two saccades of each performing saccade sequence.

Pharmacological reversible inactivation

To examine the causal role of two brain areas during the sequential saccades respectively, we applied a pharmacological reversible inactivation experiment. Reversible inactivation procedures were performed after electrophysiological recordings and microstimulation experiments. The muscimol (a $GABA_A$ agonist) would be injected primarily using a 'microinjectrode' before monkeys performed sequential saccade tasks. The 'microinjectrode' (32-gauge cannula) was inserted into an injection site through a transdural guide tube and the neuronal responses around the injection site were detected by the recording tungsten microelectrode inside the 'microinjectrode'.[53–56]

For LIP, both the left and right hemispheres were separately inactivated. To ensure comprehensive coverage of the area, three injection sites were selected for each hemisphere injection. For Monkey E's left hemisphere, injection sites were located at AP = 3.2, DV 10000 μm from dura; AP = 0, DV 6000 μm; and AP = −3.2, DV 9000 μm. While for Monkey M's right hemisphere, sites were at AP = 2.4, DV 12000 μm from dura; AP = −0.8, DV 12000 μm; and AP = −3.2, DV 9500 μm. For each hemisphere, 3 inactivation sessions (repetitions) were conducted. For DLPFC, two injection sites were selected for each hemisphere in Monkey I, AP = 25.8, DV 6000 μm from dura; and AP = 28.2, DV 6500 μm for the left hemisphere. While AP = 25.8, DV 6500 μm and AP = 30.6, DV 7000 μm for the right hemisphere. 2 inactivation sessions (repetitions) were conducted for each hemisphere. For each site, 2 μL (10 μg/μL) of muscimol, which could inactivate a roughly spherical region with a 2 mm radius for hours,[57] would be injected at a rate of 0.1 μL/min powered by a mini pump (Longer Precision Pump Co., Ltd, TJ-4A/SL0107-1A, Hebei, China), taking a 20 min post-injection period to ensure sufficient diffusion before needle withdrawal.

To reduce the variance and ensure a more stable baseline for comparison, data collected two days before muscimol injection was named 'pre' block and used as a control. Regarding the 'muscimol' block, previous studies have indicated that muscimol can still exhibit effect up to 12 h after injection,[54,56] and in some cases, its effects may last even longer, up to 24 h.[55] Additionally, our injection process, which involved injecting muscimol into multiple sites within each brain area, took approximately 2∼3 h to complete. During this time, monkeys were required to remain seated with their heads fixed, which may have consumed physical and mental energy. Consequently, their behavior might not accurately reflect their true state immediately after injection. Therefore, the data collected 6 h after muscimol injection was named 'muscimol' block and used to analyze the causal effect of brain areas on the sequential saccade. For each session, every experiment condition ('control', or 'muscimol') contains 1∼6 blocks of trials, each block contains ∼25 trials.

Cell classification

Our purpose was to study the relationship between the neural activity of saccade-related cells and sequential saccade tasks. Therefore, we first selected 100 ms before the saccade onset as the pre-saccadic epoch, and 100 ms before the cue for the start of the first saccade as the baseline. In the LLRR and RRLL sequential saccades task, if the firing rate of the pre-saccadic epoch in at least one of the eight saccades was significantly different from baseline ($p < 0.01$, Mann-Whitney test), the cell was defined as pre-saccadic cell, then performing further analysis. To detect the hierarchical representation of DLPFC and LIP in saccade sequences, cells were further classified into four groups depending on their role in the sequence hierarchy: **Sequence**, **Subsequence**, **Element** neurons as well as **Unclassified** neurons. The criterion is as follows.

(1) **Sequence neurons.** We classified the cells that responded selectively to the start or stop of the sequences as sequence cells. If the firing rate of the 1st saccade was higher or lower than the other three in both LLRR and RRLL sequence, and this difference was significant in at least one sequence task ($p \leq 0.05$, one-way ANOVA), the cells would be classified as "Sequence

start'' neurons. Similarly, if the neuronal activities were selective to the 4th saccade in LLRR as well as RRLL, the cells would be classified as ''Sequence stop'' neurons.

(2) **Subsequence neurons.** We first defined the two saccades with the same direction as a subsequence, so that both LLRR and RRLL saccade sequences contained two subsequences, LL, and RR. Neurons in this group encode the rank information at the subsequence level, with which the firing rate of one saccade in the subsequence (LL or RR) was higher than the other saccade. Meanwhile, this difference was consistent within LLRR and RRLL sequential saccade tasks and was significant in at least one sequential saccade task ($p < 0.05$, one-way ANOVA). Subsequence neurons had two subgroups: ''Subsequence start'' neurons that preferred the 1st saccade and the ''Subsequence stop'' neurons that preferred the 2nd saccade. In cases where neurons showed characteristics of multiple types, we assigned them to one subsequence type based on their strongest preference in the LLRR sequence, indicated by the highest discharge in the sequence.

Since there was always a back saccade after a center-out saccade and the inter-saccade interval was only about 300 ms, a challenge might be raised whether the neural activity in the inter-saccade interval primarily reflects the post-saccadic activity of the preceding saccade or the pre-saccadic activity of the upcoming saccade. Therefore, we applied additional analysis for the Subsequence stop neurons (there were no back saccades before the first saccade for the Subsequence start neurons). We first found the peak time of the neuronal activity between the preceding saccade onset and upcoming saccade onset for every trial, and calculated the response peak of the preceding saccade ($RP_{preceding\ saccade}$, the period between preceding saccade onset and the peak time) and response peak of the upcoming saccade ($RP_{upcoming\ saccade}$), respectively. Then we compared the variability (Standard Deviation, σ) of the $RP_{preceding\ saccade}$ and $RP_{upcoming\ saccade}$ across trials. If $\sigma_{upcoming\ saccade}$ was smaller than $\sigma_{preceding\ saccade}$, indicating a better alignment of the burst with the upcoming saccade; If $\sigma_{preceding\ saccade}$ was smaller than $\sigma_{upcoming\ saccade}$, indicating a better alignment of the burst with the preceding saccade. Finally, we removed the neurons shown more relevant to the preceding saccade.

(3) **Element neurons.** Neurons at the element level encoded one basic characteristic of saccades in our study: direction. Cells belonging to Element neurons followed two criteria. First, the firing rate of neurons between two same-direction saccades (1st L vs. 2nd L and 1st R vs. 2nd R) had no significant difference ($p < 0.05$, one-way ANOVA with Tukey's multiple comparisons test) from each other in both the LLRR and RRLL sequential saccade tasks. Second, if the average firing rate of one direction (left or right) was significantly higher than another (averaged L vs. averaged R, $p < 0.05$, paired t-test), the significant direction needs to be the same across both the LLRR and RRLL sequential saccade tasks. Then Element neurons could be further classified into three subgroups: Element neurons that preferred the leftward saccade (Element left) and the rightward saccade (Element right) respectively, as well as cells with the average left-direction firing rate had no significant difference to the average right-direction firing rate ($p < 0.05$, paired t-test) in two sequential saccade tasks (Element same).

(4) **Unclassified neurons.** Neurons that could not be classified into the former three groups were named Unclassified neurons as those neurons always discharged disparately across the LLRR and RRLL sequential saccade tasks.

QUANTIFICATION AND STATISTICAL ANALYSIS

Statistical analyses were performed using GraphPad Prism 8.0.1 (GraphPad) or MATLAB R2016b. Comparisons of neuronal activities were performed by one-way ANOVA with Tukey's multiple comparisons test. Comparisons of neuron percentage or trial percentage were performed by Fisher's exact test. The correct rate, initiation latency, or sequence duration of microstimulation experiments were analyzed by paired t-test. The correct rate change, initiation latency change, or sequence duration change of inactivation experiments were analyzed by one sample t-test. Error bars represent the mean ± SEM. *p* values less than 0.05 were considered significant, $^{*}p < 0.05$, $^{**}p < 0.01$, $^{**}p < 0.001$.